Caroline Gamerith BSc

Bioactive multilayer coatings for prevention of bacterial biofilm formation on indwelling medical devices

Masterthesis

A thesis submitted in partial fulfillment of the requirements for the degree of Master of Science in „Biotechnology"

Institute of Environmental Biotechnology
Graz University of Technology

Supervisor: Prof. Georg Gübitz
Supervisor: Prof. Tzanko Tzanov
Supervisor: Dr. Margarida M. Fernandes

Graz, November 2012

“I am among those who think that science has great beauty. A scientist in his laboratory is not a mere technician: he is also a child confronting natural phenomena that impress him as though they were fairy tales.”

(Marie Curie)

Abstract

Bacterial biofilm formation on indwelling medical devices is a common cause of medical infections. These biofilms are difficult to treat due to their resistance to antibiotics and consequently alternative approaches are needed. In this study, an enzyme-based multilayer was coated onto silicone films through a layer-by layer technique, using acylase and α-amylase as active agents. These enzymes were chosen according to their ability to degrade the quorum sensing signals of gram negative bacteria and the exopolysaccharide matrix formed by biofilms, respectively. In fact, both enzymes in solution showed an effective inhibition of biofilm formation by *Escherichia coli* and *Pseudomonas aeruginosa*, two of the most common bacteria in nosocomial infections. By alternate deposition of negatively charged enzymes and positively charged polyethylenimine, a 9.5 bilayer film was assembled on silicone films as proven by water contact angle, Fourier transform infrared spectroscopy (FTIR) and fluorescence microscopy of FITC labelled enzymes. The immobilized enzymes were found to be biologically active and stable after one week storage at room temperature and a 24 hours washing step at 37°C in water. Also no further changes in water contact angle and FTIR spectra were observed after this 24 hours washing step. The bioactive coating on catheters showed promising results in a biodynamic biofilm inhibition test. In addition these results suggest that this enzyme-based coating is stable, bioactive and can be further used to counteract biofilm formation on indwelling medical devices.

Kurzfassung

Die Bildung von bakteriellen Biofilmen auf medizinischen Implantaten ist ein häufiger Grund für Infektionen. Da Biofilme resistent gegen Antibiotika sind und daher schwierig zu behandeln sind, ist es notwendig alternative Strategien zu entwickeln.

In dieser Arbeit wurde eine mehrlagige Beschichtung mit Enzymen auf Silikonstreifen mittels „layer-by-layer“ Technik gebildet. Die verwendeten Enzyme Acylase und α-Amylase sind dabei die aktiven Wirkstoffe. Diese Enzyme wurden bezüglich ihrer Fähigkeiten ausgewählt die von Gram negativen Bakterien freigesetzten quorum sensing Moleküle zu eliminieren (Acylase) oder die von Biofilmen gebildete Exopolysaccharid Matrix abzubauen (α-Amylase). Beide Enzyme konnten in Lösung (in nicht-immobilisierter Form) die Biofilmbildung von *Escherichia coli* und *Pseudomonas aeruginosa*, zwei der häufigsten Erreger nosokomialer Infektionen, inhibieren. Durch alternierende Schichten von negativ geladenen Enzymen und positiv geladenem Polyethylenimin wurde ein Film bestehend aus 9.5 Doppelschichten auf Silikonstreifen aufgebaut. Der erfolgreiche Aufbau dieses Films wurde durch Methoden wie „water contact angle“, FTIR Spektrometer und Fluoreszenz Mikroskopie von FITC-markierten Enzymen nachgewiesen. Es konnte gezeigt werden, dass die immobilisierten Enzyme biologisch aktiv sind, sogar nach einer einwöchigen Lagerung bei Raumtemperatur, sowie nach einem 24 Stunden Waschschritt bei 37 °C. Es wurden auch keine weiteren Veränderungen des „water contact angle“ oder der FTIR Spektra nach diesem 24- stündigen Waschschritt beobachtet. Diese bioaktive Beschichtung auf Kathetern zeigte vielversprechende Ergebnisse in einem dynamischen Biofilminhibierungstest.

All diese Ergebnisse deuten darauf hin, dass diese Enzym-basierende Beschichtung stabil und enzymatisch aktiv ist und so zukünftig für die Inhibierung von Biofilmbildung auf medizinischen Implantaten eingesetzt werden kann.

STATUTORY DECLARATION

I declare that I have authored this thesis independently, that I have not used other than the declared sources / resources, and that I have explicitly marked all material which has been quoted either literally or by content from the used sources.

…… ……..

date (signature)

Acknowledgments

First of all I would like to thank Prof. Georg Gübitz and Prof. Tzanko Tzanov who gave me the opportunity to write my diploma thesis and work on an international project.

Special thanks go to my supervisor Margarida Fernandes who always helped me with words and deeds.

Thanks to the whole GBMI group (Toni, Carlos, Mari, Teresa, Eva, Sundar, Guillem, Diana, Mercè, Sonia and Kristina) for your support in the lab as well as for having a nice time in Terrassa.

Furthermore I want to express my gratitude to my whole family because they have always supported me in all kinds of way.

Last but not least thanks to my boyfriend Andreas for the outstanding support in the last years!!

Thank you!

Abbreviations

µg	Microgram
AHL	acyl homoserine lactone
APTES	(3-aminopropyl)-triethoxysilane
BCA	bicinchoninic acid
bp	base pair
CV	crystal violet
DI H_2O	deionized water
EtOH	Ethanol
FITC	fluorescein isothiocyanate
g	Gram
HSL	homoserine lactone
LbL	layer-by-layer
mg	Milligram
min	Minute
ml	Millilitre
mM	Millimolar
ms	Milliseconds
MH	Müller Hinton
NaPB	sodium phosphate buffer
nm	Nanometer
OD	optical densitiy
ONC	overnight culture
PBS	phosphate buffered saline
PEI	Polyethylenimine
SDS	sodium dodecyl sulphate
Sln	Solution
Std	Standard
U	Unit
UTI	urinary tract infections

Contents

I. Introduction

1. Introduction

More than 60 % of bacterial infections currently treated in hospitals are caused by bacterial biofilms [1]. These biofilms are difficult to treat due to their resistance to antibiotics [2; 3].
Bacterial biofilms and the concomitant encrustation of the catheters lead to big problems in catheterization. The catheters have to be changed regularly, which causes high medical costs and uncomfortable procedures for the patients. Furthermore biofilms on urethral catheters are often the reason for urinary tract infections [4; 5]. Alternative approaches are needed to counteract these biofilms. Evolutionary pressure on bacteria promotes the resistance development. Therefore, new approaches against biofilms should only target the formation of the biofilm and not the viability of the bacterial cells [6].

Enzymes are already widely used in the industry and show a lot of advantages, as most enzymes are cheap, biocompatible and environmental-friendly [7].

Our objective is to use enzymes that interfere with different steps of the biofilm formation. With these enzymes we want to achieve a bioactive multilayer coating on silicone surfaces to avoid biofilm formation on medical indwelling devices, such as catheters.

II. Theoretical Background

1. Biofilms

1.1 Definition of biofilms

Biofilms are a ubiquitous type of microbial growth in nature [8]. They are defined as complex communities of microorganisms that are attached on a surface and enclosed in a self-produced exopolysaccharide matrix. Within these three-dimensional structures the bacteria are organized as communities with functional heterogeneity [9]. The formation of a biofilm allows the bacteria to survive in a hostile environment; they are protected from the immune system and environmental stresses. Furthermore biofilms show an increased resistance to antimicrobials (e.g. antibiotics) in comparison with their planktonic counterparts [10]. Reasons for this increased resistance to antibiotics are the penetration barrier that biofilms may present to antimicrobials and the rapid efflux of antimicrobials that still manage to penetrate.

Mass transport through the biofilm is very important, because it's often a rate limiting process. The nutrient supply within a biofilm occurs through channels that are connected with the bulk liquid. Voids in biofilms can increase the velocity of substrate and product exchange with the bulk liquid [11].

It's also known that bacteria express different genes in different stages and regions of a biofilm [12]. Because of this complex structures and metabolisms biofilms have been compared to tissues of higher organisms [10].

1.2 Significance of biofilms

Due to their resistance to the immune system and antibiotics, biofilms are a common cause of difficult-to-treat medical infections associated with medical indwelling devices such as catheters [2; 13].

About 50% of the two million cases of annual nosocomial infections in the United States are associated with indwelling devices and their direct medical costs exceed $3 billion per year [1]. Approximately 40 % of all nosocomial infections are urinary tract infections (UTI) caused by biofilms on catheters [14; 15; 16].

Therefore catheter-associated UTIs are the most common hospital-acquired infections. Usually UTIs are benign, but in 2-4% of the patients they cause a bacteremia and lead to a three times higher fatality rate [14; 17]. A single bacterial species or a mixture of bacterial species and fungi can cause these biofilm infections [9]. Bacterial biofilm cells release antigens and stimulate the human body to produce antibodies. But within biofilms these antibodies cannot effectively kill bacteria instead they can damage the surrounding tissues [18]. Even patients with excellent immune reactions can rarely resolve a biofilm infection by their own defence mechanisms [19].

The resistance of biofilms to antimicrobials and their involvement in indwelling-device- related infections made it necessary to search for coatings or surfaces that prevent the formation of biofilms [9].

1.3 Formation of biofilms

Biofilm formation is a dynamic process that is divided into five distinct developmental stages that occur in a cyclic manner. figure 1 shows an overview of the different steps in the formation of a biofilm. In the beginning the bacteria grow as planktonic cells. When getting in contact with a surface or interface the planktonic cells become associated with the surface. This leads to the second step, the formation of a monolayer. At this stage the biofilm formation is still reversible, so the cells can easily detach or move along the surface. In the third step of biofilm formation the bacteria become irreversibly attached and start to form microcolonies. Different forces and interactions, such as specific adhesive forces, hydrogen bonds, van der Waals forces and hydrophobic interactions are responsible for this attachment. The fourth and last step in the formation of a mature biofilm is associated with the production of an extracellular polysaccharide matrix (EPS). This EPS, which is secreted by the cells into their environment, mainly consists of sugar residues and is essential to build the characteristic three-dimensional structure. Through detachment and breaking up the bacteria can return to their previous planktonic status, which is also important for the maintenance of a mature biofilm.

To progress to the next biofilm developmental stage the bacteria have to express particular genes. In addition to these genetic requirements also environmental and physical conditions have an influence on biofilm formation [20; 21].

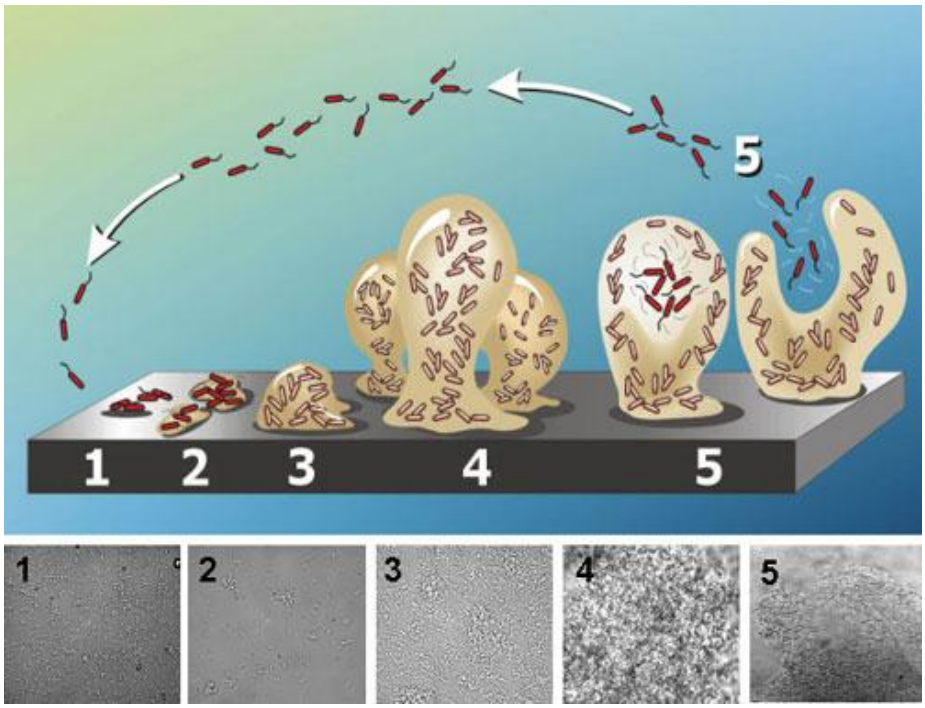

Figure 1: Stages of Biofilm Development.

5 steps in biofilm formation: initial attachment, irreversible attachment, maturation 1, maturation 2 and finally dispersal. Lower part: electron micrographs of a *P. aeruginosa* biofilm at each step **[63]**. (Image Credit: D. Davis)

Not only which species will be able to form a biofilm, also the maximum biofilm thickness and density are under great influence of environmental factors such as nutrient sources and conditions such as pH, osmolarity, temperature, oxygen and surface properties. Different organisms require diverse conditions to build a biofilm. Even different strains of the same bacterium can have diverse requirements. For example some *E. coli* strains only form biofilms under starvation conditions while other strains require high sugar and osmolarity. The model organism used for biofilm studies *P. aeruginosa* forms biofilms under most nutrient and environmental conditions. Physical properties that affect biofilm formation are hydrodynamic and physico-chemical characteristics. The most important physico-chemical characteristic is the roughness of the surface.

According to these facts biofilms differ particularly depending on their environment and the surface. For example biofilms on orthopaedic prosthesis without constant flow will differ from those on catheters under regular urine flow [20].

1.3.1 Composition of EPS:

The presence of the extracellular polysaccharide matrix (EPS) is essential for biofilm formation and maintenance. The EPS surrounds the bacteria in biofilms and protects them from different factors, such as environmental stresses and host immune responses. Although the EPS is omnipresent in biofilms its composition can greatly vary. The main components are exopolysaccharides, proteins and DNA. Furthermore outer membrane proteins and different cell appendages, for example pili and flagella, can be part of the matrix. Normally the biofilm components are self-produced.

The main polysaccharides of *E. coli* and *P. aeruginosa* will be explained now.

E. coli is able to synthesize cellulose, colanic acid, capsular polysaccharides and poly-N-acetyl-glucosamine (PGA). The disruption of the gene which is responsible for the expression of PGA was found to severely decrease the biofilm formation in a microtiter plate assay. Unbranched poly-1,6-N-acetylglucosamine with less than 3 % non N-acetylated glucosaminyl moieties and without major substitutions builds *E. coli's* PGA. There is also a group of surface proteins in *E. coli*, called self-associating autotransporters (SAAT) that promote the cell aggregation and biofilm formation.

P. aeruginosa strains are able to produce at least three different polysaccharides, namely alginate, PEL and PSL. Alginate is an exopolysaccharide and is a linear copolymer of β-1,4-linked D-mannuronic acid and L-guluronic acid residues. Alginate is responsible for the mucoid phenotype of late-stage cystic fibrosis disease.

The main difference between PEL and PSL is the main component. PEL consists mainly of glucose, whereas PSL's major component is mannose. But their common ground is that they are both branched heteropolysaccharides.

A static attachment assay showed that PSL and PEL are important for different stages in the development of a biofilm. PSL plays a major role in the early stages, while the synthesis of PEL is more important in the later stages of biofilm formation [22].

2. Quorum Sensing and Regulation of gene expression in biofilms

2.1 Definition of quorum sensing

For many years bacteria have only been seen as individual cells. Recently the notion that the individual cells in a population act as heterogeneous unit has become evident. Bacterial populations have a collective behaviour that is controlled by intercellular communication networks. This enables the population to change and adapt their behaviour depending on environmental challenges. This cell-to-cell communication between bacteria is called quorum sensing (QS) and depends on so-called autoinducers. Autoinducers are small diffusible signal molecules that play an essential role in gene expression [23] [24]. The increased concentration of signal molecules in the extracellular environment is directly proportional to the increase of the bacterial cell density within a population. At a certain concentration of QS signals, the so-called threshold level, the bacterial population is “quorate” (see figure 2). This leads to the activation of a signal transduction cascade that finally ends in the expression or repression of target genes that control the community behaviour [25; 26]. This communal behaviour was first found in *Vibrio fischeri* where the bioluminescence is dependent on an autoinducing substance [27]. Later on, this autoinducing substance could be identified as acylhomoserine lactone (AHL) [28].

Now many different signalling molecules have been identified that belong to several chemical classes. These signalling molecules can be separated in two main categories: a) short peptides and amino acids normally used by Gram- positive bacteria (autoinducing peptides – AiPs) and b) fatty acid derivatives that are commonly used by Gram-negative bacteria (AHLs) [29; 30].

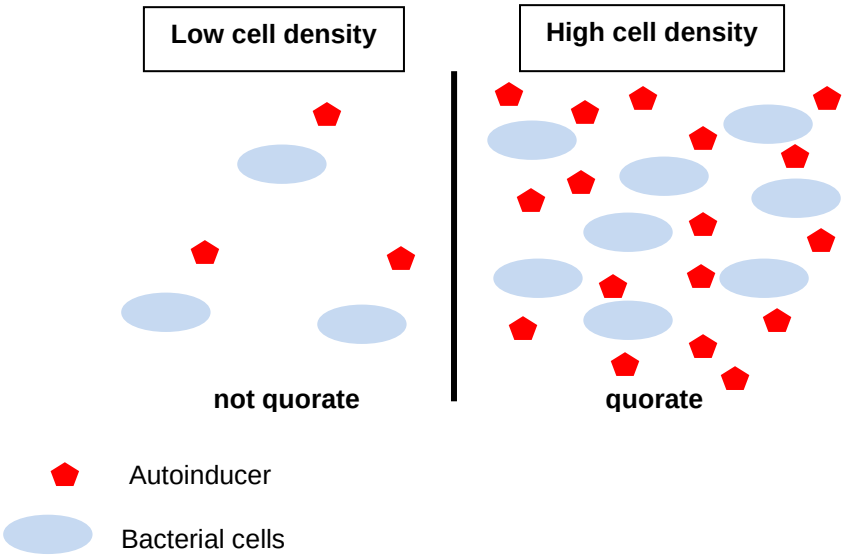

Figure 2: Principle of quorum sensing.

Only at high cell densities there are enough autoinducing molecules so that the population is quorate.

2.2 Quorum sensing in Gram-negative bacteria: LuxR-LuxI system

As most of the bacteria associated with biofilm formation on catheters are Gram-negative, e.g. *Pseudomonas aeruginosa, Escherichia coli* and *Proteus mirabilis*, this chapter will explain the quorum sensing system in Gram-negative bacteria.

After the first discovery of the AHL in *Vibrio fischeri,* variant AHL signals with different length and substitutions have been identified in a number of Gram-negative bacteria. The basic composition is a lactonized homoserine that is ligated to a fatty acyl chain through an amide bond. The length of the acyl chain can vary between 4 and 16 carbons and the third carbon in the acyl chain can carry a hydroxyl group, which can be a fully oxidized carbonyl or be fully reduced [29; 30].

Figure 3 shows the structure of the AHL core molecule as well as some examples for different bacteria.

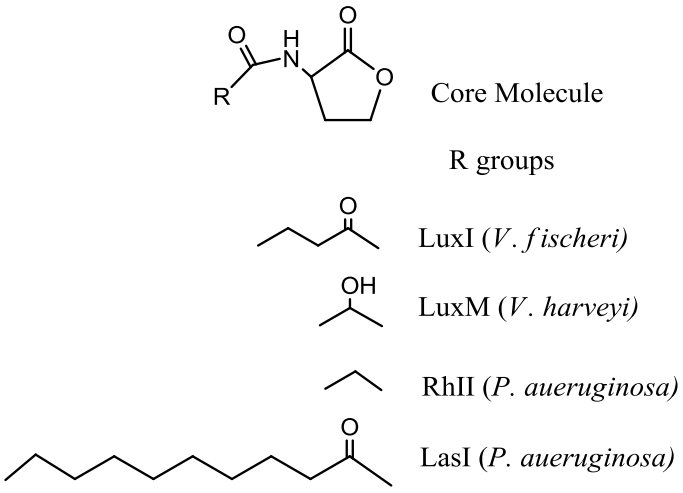

Figure 3: Acyl - homoserine lactones.
The core molecule and some examples from different bacteria

Figure 4 shows the principle of the LuxR-LuxI quorum sensing system. The gene *luxI* codes for the LuxI protein that synthesizes the QS signal AHL. AHL is diffusible and can cross biological membranes [31; 32]. The signal receptor LuxR, encoded by a gene called *luxR*, is an AHL dependent transcriptional activator. LuxR is not a trans membrane protein, but stays in the cytoplasm. Once AHL is bound to LuxR this complex binds to the RNA, interacts with the RNA polymerase and triggers the transcription of the operon. The LuxR-AHL complex induces the expression of the target genes [30].

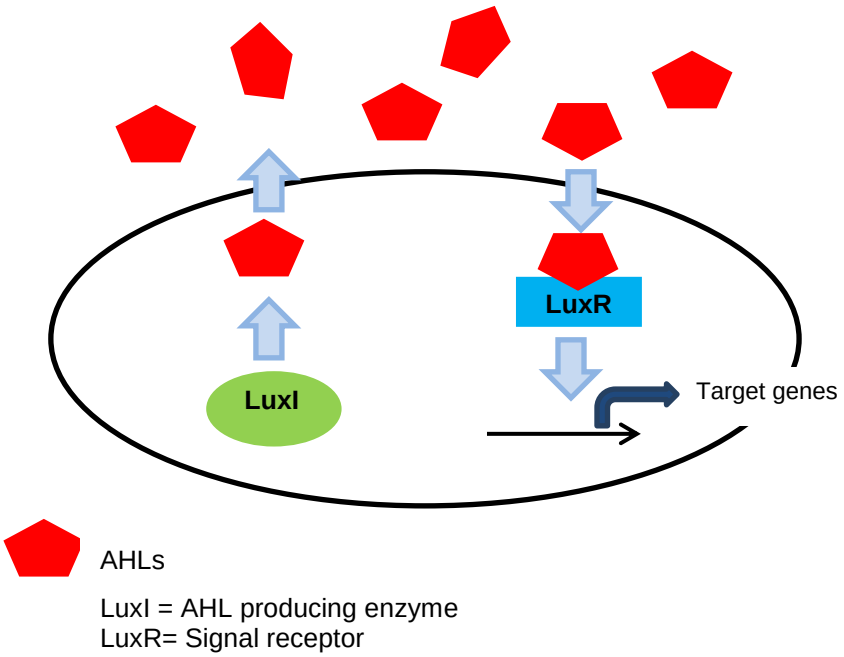

Figure 4: General principle of the LuxR- LuxI quorum sensing systems.
AHL signalling molecules produced by LuxI can bind to receptor protein luxR and induce the expression of target genes.

2.2.2 *Vibrio fischeri and its bioluminescence as a QS model*

Vibrio fischeri is a Gram - negative bacterium that can be found in marine environments. Its bioluminescence is caused by transcription of the Lux operon that contains the *luxI* gene, five genes that are essential for bioluminescence (*lux*CDABE*)* and one gene which function is not yet clear (*lux*G). The three genes *lux*C, *lux*D and *lux*E code for components of an acid reductase, an enzyme that provides the substrate for the luciferase. The genes *lux*A and *lux*B code for the two components of the luciferase (the light producing enzyme).

V. fischeri often lives in symbiosis with different fishes and squids. There the bacteria colonize the light organs and grow to very high cell densities. *V. fischeri* normally expresses *lux*I at a low level, so the concentration of AHL in the surrounding is low. If the bacteria are growing in a light organ, they reach high densities. Therefore, a high concentration of AHL is in the environment. Under these conditions the *lux* genes will be activated. First the AHL binds to the Lux receptor and then the LuxR-AHL complex binds to the *lux* box. The *lux* box is a 20 bp region about 42.5 bp from the transcription start of the first gene of the *lux* operon. The LuxR interacts with the RNA polymerase and triggers the transcription of the operon (see figure 5).

The produced light is beneficial for the animal; in exchange the bacteria receive their nutrients from the animal [30; 33; 34].

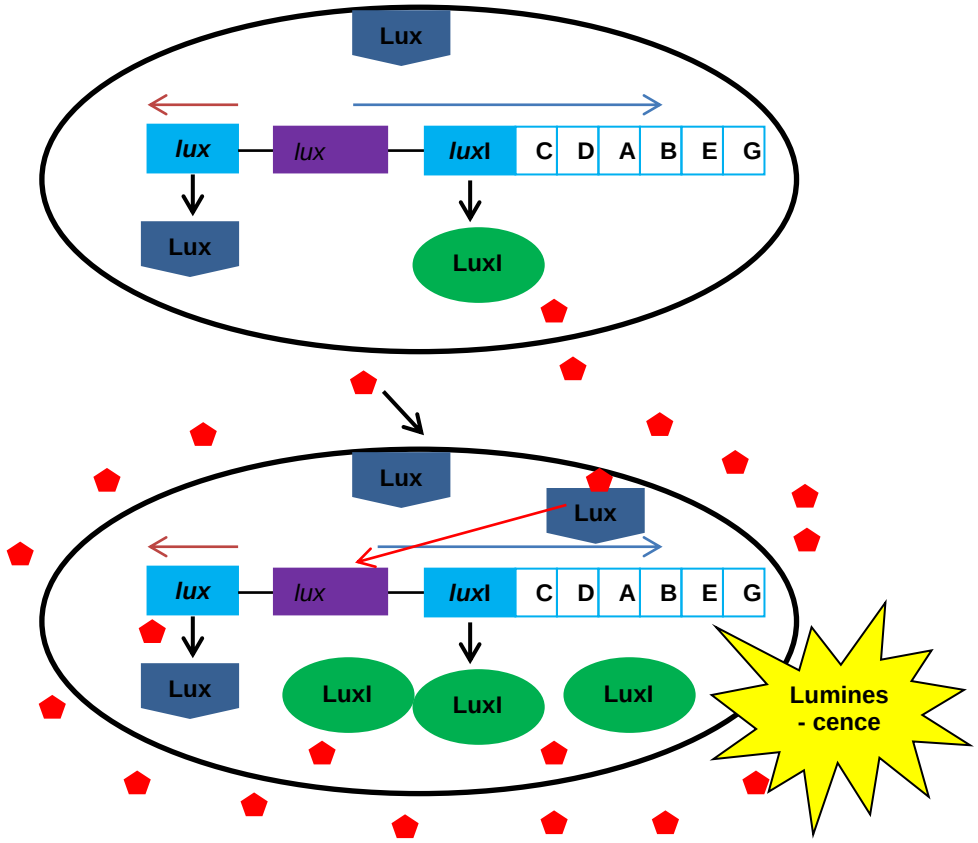

Figure 5: The regulation of bioluminescence in *V. fischeri.*

Bioluminescence is caused by transcription of the Lux operon that contains the *luxI* gene and five genes that are essential for bioluminescence. The three genes *lux*C, *lux*D and *lux*E code for components of an acid reductase, an enzyme that provides the substrate for the luciferase. The genes *lux*A and *lux*B code for the two components of the luciferase (the light producing enzyme).

2.2.3 *Quorum sensing in Pseudomonas aeruginosa*

Many bacteria use AHLs as signalling molecules and have homologues of LuxR and LuxI. Hence, the regulation itself is very similar in all these cell-to-cell communication systems, but the target genes are different.

In *P. aeruginosa* two homologues of the LuxR-LuxI system are responsible for the regulation of various genes by QS. These target genes encode a lot of different functions, including the synthesis of virulence factors, the synthesis of exoenzymes and the development of biofilms. The two *P. aeruginosa* QS systems are the LasR-LasI system and the RhlR-RhlI system [35; 36].

The LasR-LasI system regulates the expression of LasA elastase, LasB elastase, exotoxin A and alkaline protease [37; 38; 39]. The two main components are the *las*I

gene and the *las*R gene. *las*I is the autoinducer synthase gene which is responsible for the synthesis of 3-oxo-C12-HSL (*N*-[3-oxododecanoyl]-L-homoserine lactone) and *las*R codes for the transcriptional activator protein [35; 36]. The expression of *las*I is very sensitive to the concentration of the LasR/3-oxo-C12-HSL complex. Due to this preference for the *las*I promoter the initial autoinducer synthesis increases rapidly, which increases the amount of free 3-oxo-C12-HSL that can bind to LasR. This autoregulatory loop is responsible for a dramatic increase of expression of virulence genes [40].

The second QS system in *P. aeruginosa* is controlled by LuxR-LuxI homologues called RhlR and RhlI. The r*hl*I gene codes for the C4-HSL (*N*-butyrylhomoserine lactone) autoinducer synthase.
The *rhl*R gene encodes the transcriptional activator protein [41]. The C4-HSL interacts with the RhlR protein and this complex activates the expression of the *rhlAB* operon that codes for the rhamnosyl-transferase [42]. Rhamnosyl-transferase is necessary for the production of rhamnolipid biosurfactants, which allow *P. aeruginosa* to swarm over semi-solid surfaces by reducing the surface tension [43]. Also for completely induced expression of alkaline protease, pyocyanine, hydrogen cyanide, lectins and elastase a functional RhlR-RhlI system is required [29].

These two regulatory systems interact with each other. The LasRI system is in the hierarchy above the RhlRI system, because the transcriptional activation of *rhlR* is dependent on the LasR/3-oxo-C12-HSL complex. Furthermore the LasRI system also controls the RhlRI system at a posttranslational level. 3-oxo-C12-HSL can bind competitive to RhlR and therefore block the binding site for C4-HSL [44].
There are also a lot of other factors involved in this cell-to-cell communication.
The two cell-to-cell communication systems of *P. aeruginosa* and their interaction with each other are shown in figure 6. The complex regulation of the cell-to-cell signalling system and the various genes under its control highlight the importance of this system for *P. aeruginosa.*

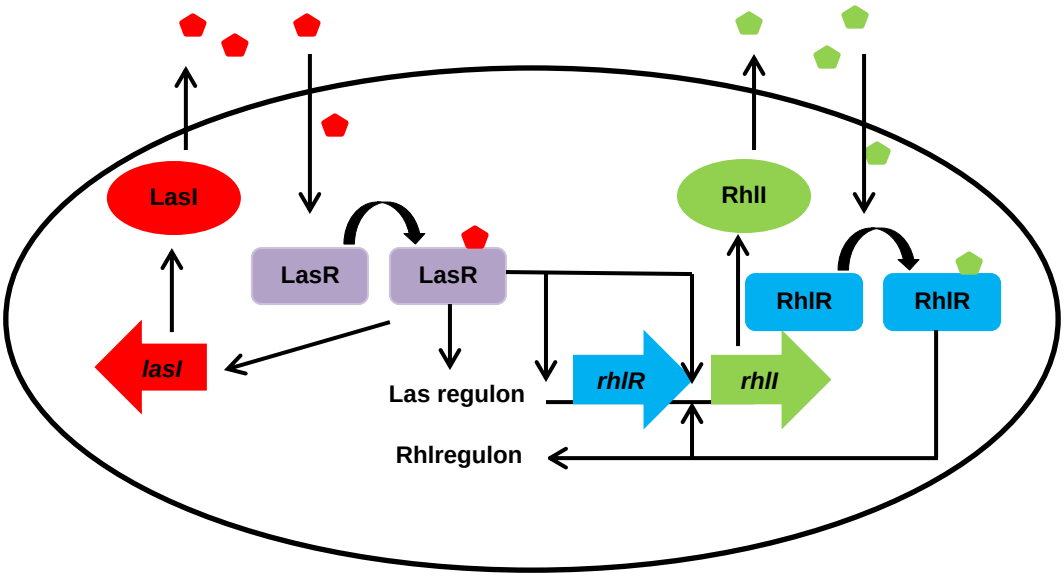

Figure 6: Interaction of the two QS systems in *P. aeruginosa*

Two homologues of the LuxR-LuxI system are responsible for the regulation of various genes by QS. The LasR-LasI system regulates the expression of LasA elastase, LasB elastase, exotoxin A and alkaline protease. The second QS system is controlled by LuxR-LuxI homologues called RhlR and RhlI. These two regulatory systems interact with each other.

2.2.4 Quorum sensing in E. coli

Although *E. coli* lacks the gene encoding the AHL synthase and is therefore not capable of synthesizing AHL molecules, it does produce an AHL receptor of the LuxR family, the so called SdiA [45]. This receptor detects AHLs from other bacteria and changes the gene expression depending on the presence of other "quorate" populations of Gram-negative bacteria.
However, *E.* coli encodes the signal-generating component of a second system, a LuxS homologue that generates autoinducer-2 (AI-2) [46].

This second system is the LuxPQ/LuxS system, where LuxS generates the AI-2 signal. AI-2 is a furanosyl borate diester, and LuxP is a periplasmic-binding protein that binds AI-2. The inner membrane sensor kinase LuxQ detects the LuxP-AI-2 complex. This system is also used from different bacteria for communication with other species. The concentration of AI-2 is supposed to give information about the total density of bacterial population in an environment [47].

2.3 Quorum quenching: Interfering with the QS system

AHL molecules have been detected in *P. aeruginosa* biofilms found in natural and clinical environments and it has been proven that the QS system plays a major role in biofilm formation and maintenance [48; 49]. Shutting down the expression of virulence genes by interfering with the QS systems has the advantage that it doesn't affect the viability of the cells. The evolutionary pressure to gain resistance would be lower compared to the pressure under antibiotic therapy [50]. Therefore, novel approaches to prevent biofilm formation and inhibition of the production of virulence factors could target the QS system [29].

The action of interfering with the QS system is called quorum quenching. As there are different components in a QS system, there are also different targets for quorum quenching. Any reagent that prevents the recognition between the QS signal and the receptor protein or the accumulation of the QS molecules themselves, might block the expression of the QS target genes. The following strategies are listed for the LuxR-LuxI type system [23].

2.3.1 Antagonists

Analogue AHLs molecules can be used as antagonists. They can bind to the LuxR receptor and block the binding site for AHL. The LuxR-antagonist complex does not proceed with the QS system pathway, so the expression of the target genes is reduced or even inhibited [51; 52].

2.3.2 Inhibition of signal biosynthesis

Another way to interfere with the QS system is to inhibit the biosynthesis of the signalling molecules. This is for example possible using the antimicrobial reagent triclosan. Enoyl- ACP reductase is an enzyme involved in the synthesis of acyl-ACP, an essential intermediate in the synthesis of AHL. Triclosan inhibits the enoyl-ACP reductase and therefore reduces the AHL production [53].

2.3.3 Signal degradation

Lactonase and acylase are two different enzymes that have been identified to degrade AHL. Lactonase hydrolyses the lactone ring of AHLs and produces the

corresponding acyl homoserines. Conversely, acylase cleaves the amide bond of AHLs and leaves fatty acids and homoserine lactone as products (see figure 7) [23].

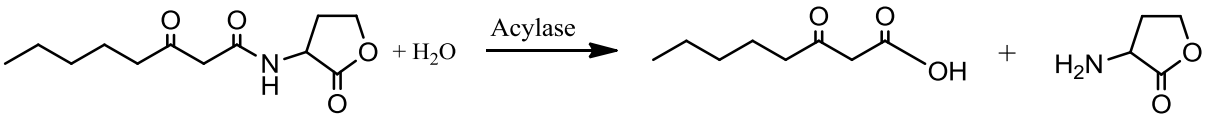

Figure 7: Quorum quenching mechanism of acylase. (AHL degradation)
The acylase cleaves the amide bond of AHLs and releases homoserine lactone and fatty acids as products.

3. Enzymes

Enzymes are very specific biocatalysts and increase the rates of chemical reactions. Most of the known enzymes are proteins, but there also exist ribozymes, catalytically active ribonucleic acids. Like all catalysts, enzymes lower the activation energy of a reaction but are not consumed by the reactions they catalyse, nor do they alter the equilibrium of these reactions.

3.1 Enzyme classification

With the enzyme commission number (EC number) enzymes are classified in 6 main categories, according to their distinct reaction types (see table 1).

Table 1: Enzyme classification

EC #	Enzymatic class
EC1	Oxidoreductases
EC2	Transferases
EC3	Hydrolases
EC4	Lyases
EC5	Isomerases
EC6	Ligases

Depending on the exact chemical reaction catalysed by an enzyme there also exist sub- and sub-subclasses [54].

3.2 Enzyme kinetics

At first the enzyme reacts with the substrate to build an enzyme-substrate complex. Then in turn this complex is converted to the product and the free enzyme again [54].

$$E + S \underset{k_{-1}}{\overset{k_1}{\leftrightarrow}} [ES] \overset{k_2}{\rightarrow} E + P$$

Equation 1: Simplification of an enzyme reaction

(E= enzyme; S= substrate; [ES] = enzyme-substrate complex; P= product; k_1, k_{-1} and k_2 are the specific rate constants for each reaction)

3.2.1 Michaelis Menten kinetics

The most common and simplest model used to describe the enzyme kinetics is the Michaelis Menten kinetic. Figure 8 shows the dependence of the reaction rate on the substrate concentration.

The reaction rate increases with increasing substrate concentration [S]. The maximum rate [v_{max}] is reached, when all enzyme molecules are bound to substrate molecules. The rate constant k_2, which is also called k_{cat} is the turnover number. K_{cat} gives the maximum number of substrate molecules converted into product molecules per molecule of enzyme per second. K_m is the Michaelis Menten constant and defines the substrate concentration at which the enzyme works with half-maximum velocity (1/2 v_{max}). K_m gives information about the substrate's affinity to the enzyme, so a small K_m indicates a high affinity, because the maximum rate v_{max} will be obtained more quickly. K_m is specific for an enzyme and substrate and also dependent on other conditions such as temperature and pH [54].

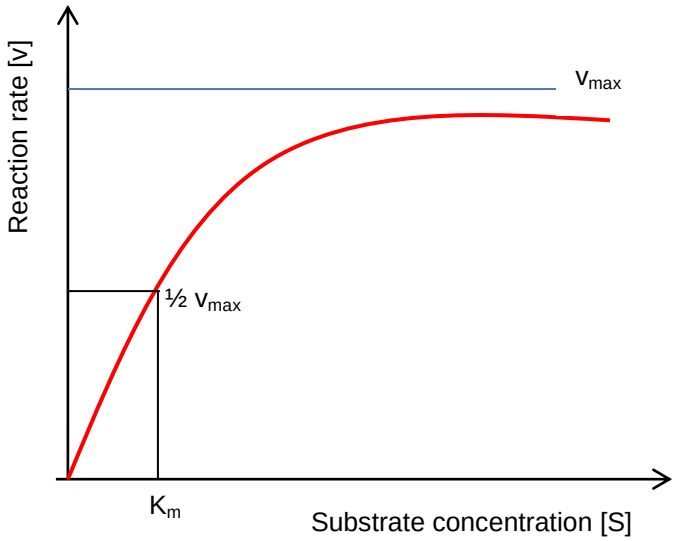

Figure 8: Dependency of the reaction rate of an enzyme as a function of the substrate concentration.

Michaelis Menten kinetics: K_m is the Michaelis Menten constant and defines the substrate concentration at which the enzyme works with half-maximum velocity (1/2 v_{max}).

The Michaelis Menten equation is given in equation 2.

$$v_0 = \frac{v_{max} * [S]}{(K_m + [S])}$$

Equation 2: **Michaelis Menten equation**

Table 2: Abbreviation and explanations for Michaelis Menten equation 2

Abbr.	Explanation
V_0	velocity of enzyme reaction [U/mg]
v_{max}	maximal velocity of enzyme reaction [U/mg]
K_m	substrate concentration at $v = \frac{vmax}{2}$[mM]
[S]	substrate concentration [mM]

3.3 Enzymes used throughout the work

3.3.1 Acylase

Acylase I from *Aspergillus melleus* is an aminoacylase and is classified as EC 3.5.1.14. Aminoacylases catalyse the chemical reaction of N-acyl-L-amino acid and H_2O as substrates to yield a carboxylate and an L-amino acid as products.

The optimum temperature for this enzyme is about 40-45°C. Acylase is stable from pH 6-10; the pH optimum is at pH 8. The enzyme is activated by $CoCl_2$ in the range of 10^{-4} to 10^{-3} M.

There is no entry in any database about the structure of acylase I from *Aspergillus melleus*. The only PDB entry for EC 3.5.1.14 is from a human aminoacylase.

3.3.2 α- amylase

α-amylase from *Bacillus amyloliquefaciens* is classified as EC 3.2.1.1. This enzyme hydrolyses alpha bonds of large, alpha-linked polysaccharides, such as starch and glycogen, yielding glucose and maltose. α-amylase from *B. amyloliquefaciens* is an endoamylase and randomly hydrolyses α-(1→4)-glycosidic linkages in amylose and amylopectin. The breakdown products are oligosaccharides and dextrins of varying chain length. The enzyme is active at high temperatures (70−90 °C).

The α-amylase from Bacillus amyloliquefaciens consists of two protein chains. Their crystal structure is shown in figure 9.

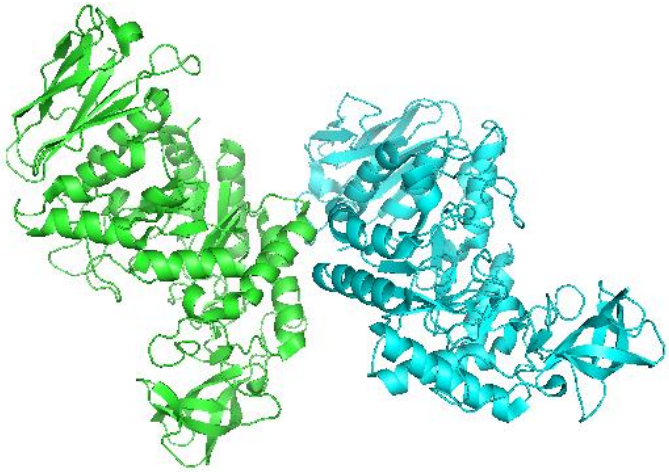

Figure 9: *Bacillus amyloliquefaciens* crystal structure [65]**.**
PDB 3bh4; The α-amylase from *B. amyloliquefaciens* consists of two protein chains

4. Layer-by-Layer technique

The layer-by-layer (LbL) technique has been widely used to produce nanofilms for biomedical applications. It‘s an easy and inexpensive adsorption technique to form multilayers on various supports. The assembly of the multilayer film is achieved by depositing alternating layers of a polyanion and a polycation on the surface. Therefore,the main forces in the film are electrostatic interactions.

Figure 10 shows the principle of such a build-up. The film is produced by alternately dipping in oppositely charged solutions with washing steps in between (see figure 10 A).The first two adsorption steps starting from a negatively charged support are shown in figure 10 B.

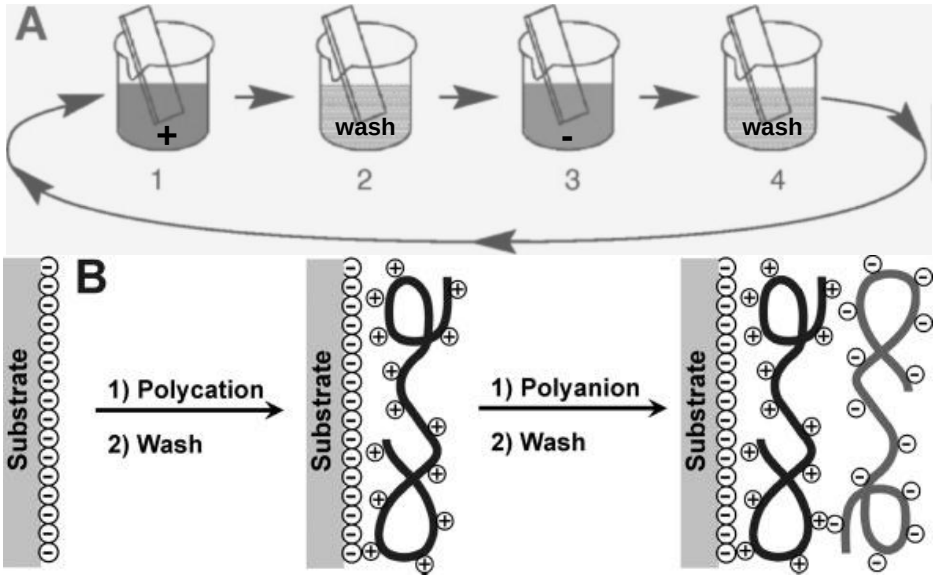

Figure 10: Principle of the layer-by-layer assembly [55].

Alternately dipping in a polycationic solution and a polyanionic solution with washing steps between them leads to the assembly of a multilayer film.

Examples for positively charged polyelectrolytes are poly(diallyldimethylammonium chloride) (PDDA), poly(allylamine hydrochloride) (PAH) or polyethyleneimine (PEI). As polyanion poly(styrenesulfonate) (PSS), poly(vinyl sulfate) or poly(acrylic acid) can be used.

For example, when a negatively charged surface is immersed in a solution of PEI and afterwards placed in a solution of PSS with washing steps between to remove the unadsorbed or loosely adsorbed polyelectrolytes, this leads to a bilayer. By repeating this procedure in a cyclic manner the build-up of a multilayer film can be achieved. Nevertheless, the LbL technique is not limited to the use of polyelectrolytes; almost all kinds of charged materials can be used for the assembly. A great number of studies have been performed with various charged components, including nanoparticles, DNA, viruses, polysaccharides, nanotubes, organic dyes and proteins. The ability to use a lot of different components and the freedom in the number of layers leads to a wide variety of structural and functional properties [56; 57].

Electrostatic interactions are not the only forces that play a role in the LbL build-up. Studies showed that also hydrogen bonding, hydrophobic interactions, charge transfer, covalent bonding and biological recognition can force the assembly. Furthermore not only charged inorganic substrates can be used as supports, also hydrophobic polymer surfaces can serve as scaffolds. A number of parameters, such

as ionic strength and pH of the deposition solutions, affect the assembly and stability of the film fabrication.

Different enzymes have been immobilized in a LbL-fashion without losing their bioactivity. One application field of enzymes in LbL assemblies is the preparation of biosensors. The LbL technique was also used for implantable materials, to achieve anti-biofouling, anti-adhesion or antibacterial properties. Therefore, our approach intends to produce a LbL film with integrated bioactive enzymes to achieve anti-biofilm or anti-biofouling materials [56].

III. Materials and Methods

1. Materials

All chemicals used were of analytical grade and purchased from Sigma-Aldrich.

Table 3: List of devices used

Devices	Company	Comments
96- well polystyrene plates	Nunc	
96-well suspension culture plates, sterile	Greiner-bio one	
CARY 1E UV-Visible spectrophotometer	Varian	For bacterial OD_{600} measurements
Drop Shape Analysis System DSA100: water contact angle	Krüss	
Scanning electron microscopy FE SEM, Quanta 200 FEG	FEI Company, USA	
Eclipse Ti-S Microscope	Nikon	
Helios γ spectrophotometer	Thermo electron corporation	For enzyme activity tests
Infinite M 200 plate reader	Tecan	
PD 10 columns G-25M	GE Healthcare	
Petri dishes	Rubilabor	
Spectrophotometer cuvettes 1.5 ml	Sudelab	
Spectrum 100 FT-IR	Perkin Elmer	

Table 4: List of bacteria, media and enzymes used

Bacteria	Supplier	Reference
Escherichia coli CECT 101		
Pseudomonas aeruginosa CECT 110		
Media		
Cetrimide agar	Sigma-Aldrich	22470 Fluka
Chromatic Coli/Coliform agar	Liofilchem	610610
Müller Hinton broth	Sigma-Aldrich	70192 Fluka
Enzymes		
acylase I from *Aspergillus melleus* [EC: 3.5.1.14]	Sigma-Aldrich (Fluka)	Lot Nr.: 1348941V
α- amylase from *Bacillus amyloliquefaciens* [EC: 3.2.1.1]	Sigma-Aldrich (Novozyme Corp.)	Lot Nr.: 120M1543V

2. Enzyme characterisations

2.1 Protein content quantifications

The protein content of the acylase powder and the amylase solution was determined with the Bicinchoninic Acid (BCA) Protein Assay Kit (Sigma).

The principle of the BCA assay relies on the formation of a Cu^{2+}- protein complex in alkaline conditions, which is followed by a reduction of the Cu^{2+} to Cu^{1+}. The amount

of reduction is dependent on the protein content. Cu^{1+} is forming a purple complex with BCA, which has an absorbance maximum at 562 nm. This absorbance is proportional to the protein concentration.
The kit consists of two reagents, the BCA solution and a 4 % (w/v) copper(II)sulfate solution. Different concentrations of bovine serum albumin (BSA) were used as protein standard.

To achieve the BCA working solution the two reagents were mixed in a ratio of 50:1. This BCA working solution was then mixed with the samples or the standard solutions in a ratio of 20:1. After incubating the samples for 20 minutes at 60°C they were allowed to cool down to room temperature. 200 µl of each sample were then transferred to a 96-well plate and the absorbance at 562 nm was measured using the Infinite M 200 plate reader.

2.1.3 Acylase protein content

For the protein content determination of acylase two different concentrations of powder were prepared, one containing 1 mg powder per ml and the other one 0,5 mg powder per ml. The BCA assay was performed as in the basic protocol and the determination of both solutions was done in triplicate.

2.1.4 Amylase protein content

For the protein content determination of amylase two different dilutions of the enzyme solution were prepared. The BCA assay was performed as in the basic protocol and the determination of both solutions was done in triplicate.

2.2 Enzyme activity assays

2.2.5 Acylase activity assay

The activity of acylase was determined using a colourimetric assay depending on the reaction shown in figure 11.

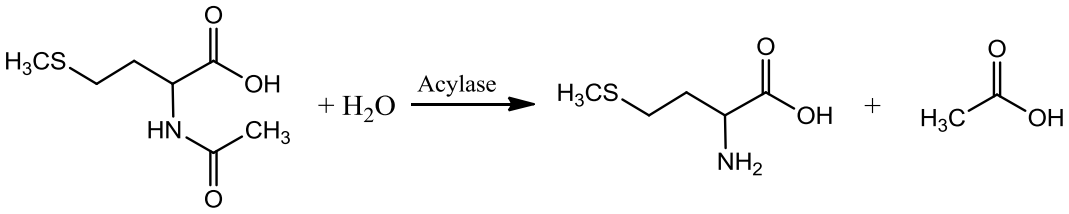

Figure 11: Acylase reaction.
N-Acetyl-L-methionine and H_2O is converted into L-methionine and acetic acid by acylase.

The produced L-methionine then reacts with ninhydrin, a chemical compound used to detect ammonia or primary and secondary amines. When reacting with the free amines of L-methionine a purple colour appears.

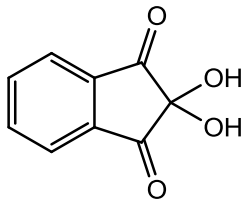

Figure 12: Chemical structure of ninhydrin.

Table 5 shows the reagents that were used for the activity determination of acylase.

Table 5: Reagents used for acylase activity assays

	Reagents
A	100 mM N-acetyl-L-methionine solution, pH 8.0 at 37°C (NAMET)
B	200 mM citrate buffer, pH 5.0 at 37°C
C	1.6% (w/v) stannous chloride solution ($SnCl_2$)
D	Ethylene glycol monomethyl ether
E	2% (w/v) ninhydrin colourreagent (NCR): in a mixture of reagent D and reagent B in a ratio of 1:1
F	50% (v/v) 1-propanol solution
G	0.5 mM cobalt chloride solution (CoCl2)
H	100 mM tricine buffer, pH 8.0 at 37°C
I	0.8 mM L-methionine standard solution (StdSoln)
J	acylase I enzyme solution: 0.1 unit/ml of acylase I in cold deionized water

For the enzymatic reaction 0.1 ml enzyme solution were mixed with 0.2 ml tricine buffer and 0.1 ml $CoCl_2$ solution. The samples were equilibrated to a temperature of 37°C for 7 minutes. Then 0.1 ml of NAMET were added and the samples were swirled. For the tests the samples got incubated at 37°C for exactly 30 min. Afterwards the reaction was stopped by incubating the tubes at 100°C for 4 min. The blanks got immediately stopped at 100°C for 4 min without prior incubation at 37°C.
After the enzymatic reaction the second step, the colorimetric ninhydrin reaction, was performed. Table 6 shows the pipetting scheme for the colorimetric reaction of the tests, blanks and standard solutions.

Table 6: Pipetting scheme for colorimetric reaction for standards, blanks and acylase solutions

[ml] of:	Test	Test-Blank	Std 1	Std 2	Std 3	Std 4	Std 5	Std - Blank
Test Sln	0,1							
Blank Sln		0,1						
StdSln			0,01	0,02	0,04	0,06	0,1	
DI H_2O			0,09	0,08	0,06	0,04		0,1
NCR	0,2	0,2	0,2	0,2	0,2	0,2	0,2	0,2
$SnCl_2$	0,01	0,01	0,01	0,01	0,01	0,01	0,01	0,01

After adding all solutions the tubes were swirled and incubated at 100°C for 20 min. Before adding 1 ml of 1-propanol the samples were allowed to cool down to room temperature. The samples were then transferred to cuvettes and the absorbance at 570 nm was measured with a Helios γ spectrophotometer.

2.2.5.1 Acylase activity at different conditions

The acylase activity assay was performed at different conditions to completely characterise the enzyme. Therefore, the tests were always performed exactly as the basic protocol; each time only one parameter was changed.

Acylase activity was measured with a variation of substrate concentrations, temperatures and pH values as well as without addition of $CoCl_2$. All experiments were done at least in triplicate.

2.2.6 Amylase activity assay

The activity of α- amylase was determined using a colorimetric assay depending on the reactions shown in figure 13 and figure 14.

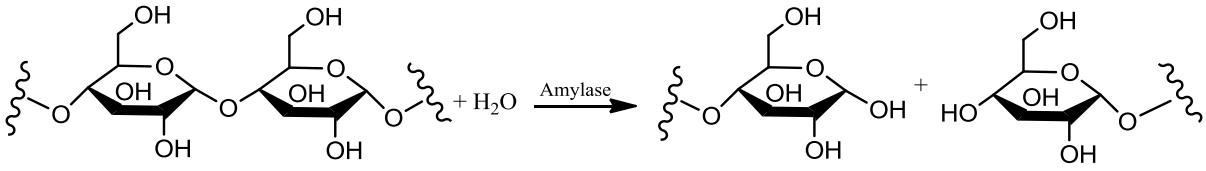

Figure 13: Reaction of α- amylase.

Poly-α-D-Glucose and H_2O are converted to maltose molecules.

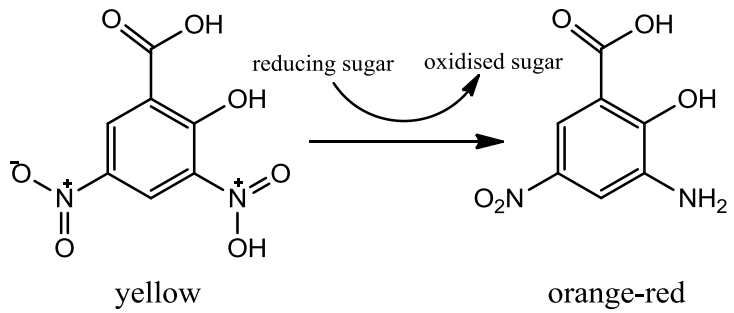

Figure 14: DNS Colour reaction.

Under alkaline conditions 3,5- dinitrosalicylic acid reacts with reducing sugars to form 3-amino,5 dinitrosalicylic acid and oxidised sugars which causes a colour-change from yellow to orange-red.

The α- amylase produces reducing sugars from starch. 3,5- dinitrosalicylic acid then reacts with the reducing sugars and forms 3-amino-5-nitrosalicylic acid, which absorbs light strongly at 540 nm.

The reagents that were used for this activity assay are shown in table 7.

Table 7: Reagents used for α - amylase activity assay.

	Reagents
A	20 mM sodium phosphate buffer with 6,7mM NaCl; pH 6,9 at 20°C
B	1,0% (w/v) soluble starch solution
C	0,2% (w/v) maltose standard
D	α- amylase solution: 1U/ml in purified H_2O
E	Colour reagent solution (ClrRgt) containing sodium potassium tartrate solution in 2 M NaOH and 96 mM 3,5- Dinitrosalicylic acid solution

For the enzymatic reaction, 0.1 ml of starch solution and 0.05 ml of enzyme solution were mixed and incubated at 20°C for 3 min. Then 0.1 ml of the colour reagent solution and 0.05 ml of enzyme solution were added and the samples were incubated for 15 min at 100°C. For the standard curve different concentrations of the standard solution were mixed with the colour reagent solution and treated the same way. Afterwards the samples were allowed to cool on ice to room temperature before being diluted 1:4 with DI H_2O.

For the blanks no enzyme solution is added before adding the colour reagent, which means that the whole amount of enzyme solution is added after the incubation time.

After mixing the absorbance at 540 nm was measured with the Helios γ spectrophotometer.

2.2.6.1 Amylase activity at different conditions

The amylase activity assay was performed at different conditions to completely characterise the enzyme. The tests were therefore always performed exactly as the basic protocol; each time only one parameter was changed.

Amylase activity was measured with a variation of substrate concentrations, temperatures and pH values. All experiments were performed at least three times.

2.3 Interference tests with both enzymes

Both enzymatic assays were also performed with a mixture of acylase and amylase to study the interaction of these two enzymes in solution.

3. Microtiter plate biofilm assay with enzymes in solution

The biofilm inhibition tests with enzyme solutions were performed with *Pseudomonas aeruginosa* and *Escherichia coli.* The bacteria were cultivated on specific cetrimide agar plates and chromatic agar plates, respectively.
Overnight cultures of *P. aeruginosa* and *E. coli* were grown in Müller-Hinton (MH) broth. These ONCs were diluted to an OD_{600} of 0.01 in fresh MH broth and grown in sterile 96-well microtiter plates. To test the biofilm inhibition of the enzymes, each well contained 135 µl of bacterial suspension and 15 µl of enzyme solution. Amylase was used in a concentration of 5.7 U/ml and acylase in a concentration of 0.2 U/ml. Negative controls were performed by adding 15 µl of buffer, tricine buffer for acylase and sodium phosphate buffer for amylase. To verify that the test works a positive control with 15 µl [100 µg/ml] of Ampicillin for *E. coli* and Gentamicin for *P. aeruginosa* was done.
Controls were performed with 150 µl of bacterial suspension without any additives. For the blanks 150 µl of MH broth were added to each well.

After incubation at 37°C for 24h the medium was gently discarded and the microtiter plate wells were washed with 200 µl of DI H_2O. Afterwards the plate wells were stained with 110 µl of 0.1 % crystal violet for 30 min at room temperature. To remove the non-bound CV solution the microtiter dish was shaken out over a waste tray and washed with 200 µl of DI H_2O. The microtiter plates were inverted and tapped on paper towels to remove any excess of liquid. Then 200 µl of EtOH (96 %) were added to each well and incubated for 10 min at room temperature to solubilize the dye. From each well 125 µl of the CV- ethanol solution were transferred to a fresh well on a 96-well-plate and the absorbance at 540 nm was measured.

This test was performed at least three times for all conditions with at least 4 replicate wells.

4. Silicone pretreatments

4.1 Silicone washing

Prior to coating the silicone was washed for 30 minutes with 5 % (w/v) sodium dodecyl sulfate (SDS). Afterwards the silicone stripes were rinsed alternately with DI H_2O and EtOH (96 %) and stored in EtOH (96 %) until further usage. The catheters were not washed prior to the coating.

4.2 Silanization with APTES

A silanization is the covering of a surface through self-assembly with organofunctional alkoxysilane molecules.
For the silanization the cleaned silicone stripes were incubated in 5 % (3-aminopropyl)-triethoxysilane (APTES) in EtOH (96 %) for 24 h at room temperature. Afterwards the silicone was washed with DI H_2O and EtOH (96 %) and stored in EtOH (96 %) until further use.

4.2.7 Ninhydrin test to prove silanization with APTES

For the Ninhydrin test dry APTES treated silicone samples were covered with a 2 % Ninhydrin solution and incubated for 20 min at 100 °C. The reaction was stopped by adding 1 ml of EtOH (96 %). Washed silicone without further treatment was used as a negative control.

5. LbL approaches

5.1 Principle LbL assembly

Different LbL approaches were performed, but the principal assembly and conditions were always the same. Acylase and amylase have an isoelectric point between pH 5 and 6. So at a pH higher than 6 both enzymes have a negative charge. As a counterpart the cationic polymer polyethylenimine (PEI) was used.

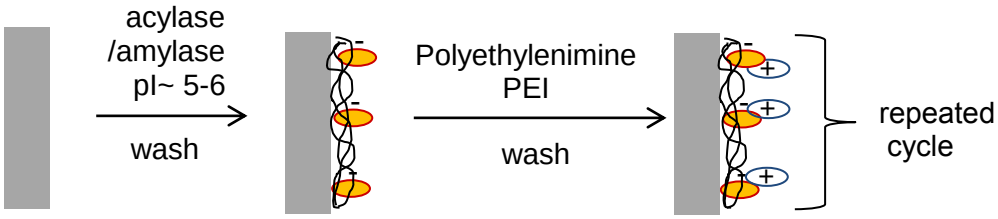

Figure 15: Scheme of LbL assembly on silicone platforms.

By alternately dipping in negatively charged enzyme solution and positively charged PEI solution with washing steps in between a 9.5 bilayer film was established.

Solutions of acylase and amylase containing 1.5 mg/ml protein in 100 mM tricine buffer pH 8 and 20 mM NaPB with 6.7 mM NaCl pH 6.9- respectively- were prepared. The PEI was used in a concentration of 3 mg/ml in the same two buffers as the enzymes. As a washing solution a 0.15 M NaCl solution with pH 8 was prepared. The deposition of the layers was achieved by dipping the silicone alternately in the oppositely charged solutions with washing steps in between. The silicone stayed in each solution for 10 min and the whole process was carried out at room temperature. This procedure was repeated to obtain the desired number of bi-layers, always ending with the enzyme solution. Afterwards a rinsing step with fresh washing solution was used to remove weakly or unabsorbed protein.

5.2 FITC labelled enzymes

5.2.1 Labelling of acylase and amylase with FITC

Enzyme solutions of acylase and amylase containing 2 mg/ml protein in 0.1 M sodium carbonate buffer pH 9 were prepared. The FITC was dissolved in anhydrous DMSO to a concentration of 1 mg/ml. For each 1 ml of protein solution 50 µl of the FITC solution were slowly added while gently stirring. After adding the required amount of FITC the samples were incubated overnight shaking at 4 °C.

Afterwards the unbound FITC was separated from the FITC-conjugate using the gravity protocol of PD-10 Desalting Columns (GE healthcare).

5.2.2 LbL with FITC labelled enzymes

To see the different behaviour of the enzymes on APTES silicone and non-pretreated silicone FITC-labelled enzymes were used to perform a LbL build-up.

The procedure described in chapter 5.1 was performed with solutions of FITC-labelled acylase and FITC- labelled amylase and repeated 5 times to obtain 4.5 bi-layers (see concept in figure 16).

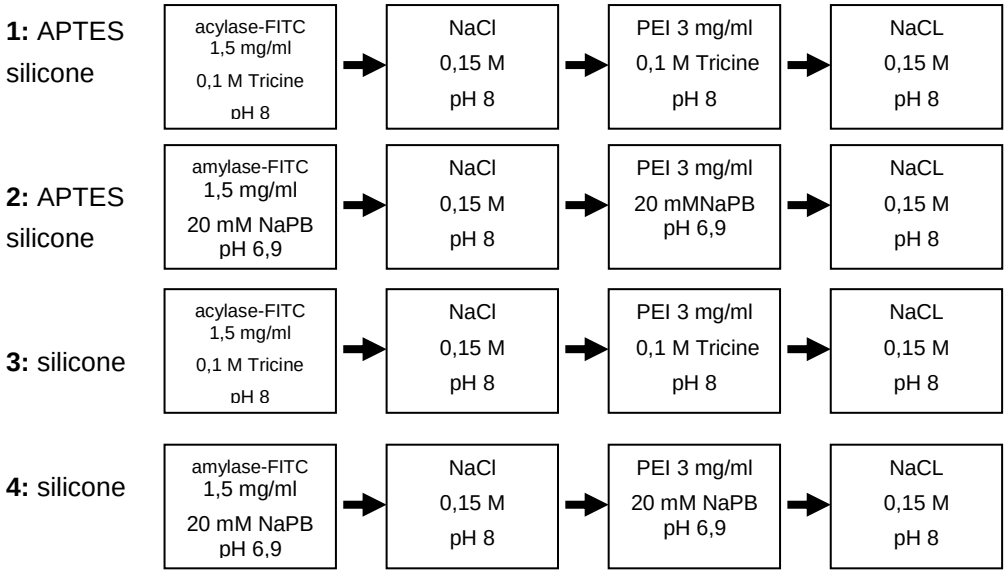

Figure 16: Concept of LbL approach with FITC-labelled enzymes.

1= LbL on APTES silicone with acylase, 2= LbL on APTES silicone with amylase, 3= LbL on silicone with acylase, 4= LbL on silicone with amylase; 4.5 bi-layers were build up in this order, the last layer was always enzyme

5.2.3 Fluorescence Microscopy of FITC-labelled LbL samples

The LbL samples with FITC-labelled enzymes were analysed using the Eclipse Ti-S microscope with UV filter.

5.3 Characterisation of LbL samples

To characterise the coatings the LbL assembly was performed again. The same procedure as in chapter 5.1 was repeated 10 times to obtain 9.5 bi-layers. Again the last layer was always enzyme. The LbL build-up was done with acylase, amylase and a combination of both enzymes (see figure 17 and figure 18) each on APTES silicone and untreated silicone.

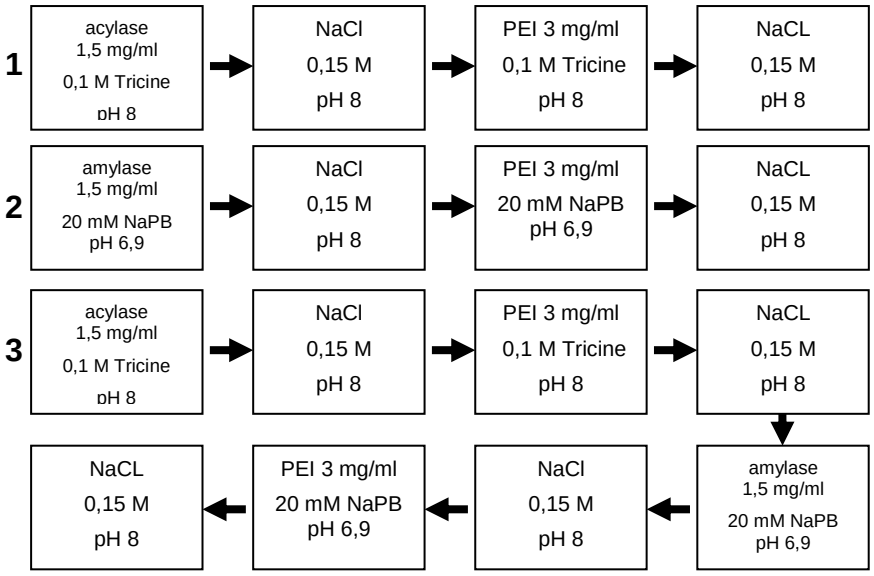

Figure 17: Concept of LbL approach.

1= LbL only with acylase, 2= LbL only with amylase, 3= LbL with acylase and amylase alternately; 9.5 bi-layers were build up in this order, the last layer was always enzyme; APTES silicone and silicone were used as supports

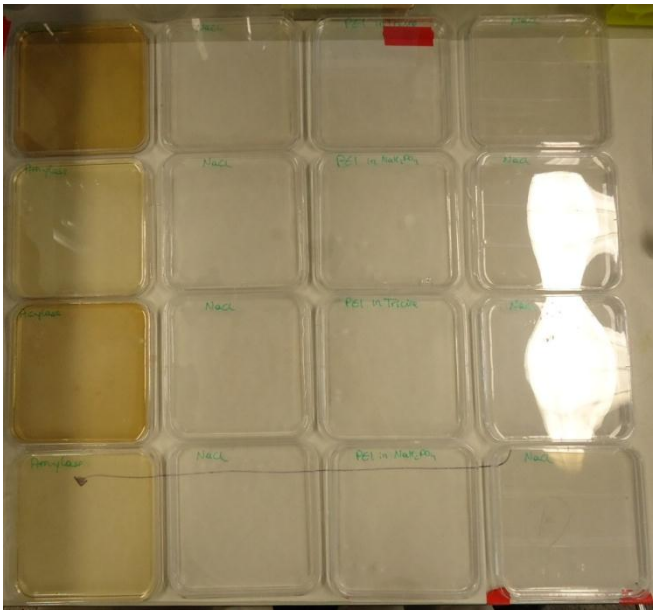

Figure 18: Construction of petri-dishes for the LbL concept as in figure 17.

To study the stability of the LbL build-up some parts of the samples were washed immediately after the assembly in DI H_2O for 24 h at 37°C and 100 rpm.

5.3.1 FTIR

The FTIR spectra were obtained using the Spectrum 100 FT-IR spectrometer.
LbL silicone and LbL APTES silicone with all 3 enzyme conditions were used as samples. To study the stability all samples were analysed again after washing 24 h in DI H_2O. Afterwards the spectra were analysed with the software “essential FTIR” (eFTIR) version 3.00.019.

5.3.2 Water contact angle

The water contact angle was measured using the Drop Shape Analysis System DSA100. The volume of the water drops was 5 µl.
LbL silicone and LbL APTES silicone with all 3 enzyme conditions and after washing 24 h in DI H_2O at 37°C were used as samples.

5.3.3 Scanning electron microscopy

To study the surface structure a blank silicone and a LbL acylase silicone (9.5 bilayers) were analysed by scanning electron microscopy (SEM) using a FESEM, Quanta 200 FEG (FEI Company, USA).

5.3.4 Enzyme activity measurements

5.3.4.1 Acylase activity

The activity of the enzyme incorporated in LbL on silicone was determined the same way as for free acylase with a few modifications (see 2.2.5). All volumes were 10 times increased and instead of free enzyme solution silicone stripes with LbL assembly were used. Instead of 1 ml only 0.4 ml of 50% 1-Propanol were added at the end. Washed silicone stripes and an assay without any enzyme served as a control and were used as blanks. Furthermore a new calibration curve with the adjusted conditions was done.
Silicone and APTES silicone with acylase or acylase and amylase incorporated by LbL were used as samples. The activity of LbL silicone samples was determined after 24 h washing in DI H_2O and after storage for 1 week.

5.3.4.2 Amylase activity

The enzymatic activity of amylase on LbL silicone was determined the same way as for free amylase, with a few modifications (see 2.2.6 and 2.2.5).
All volumes were 10 times increased and instead of free enzyme solution silicone stripes with LbL assembly were used. Washed silicone stripes and an assay without any enzyme served as a control and were used as blanks. Silicone and APTES silicone with amylase or acylase and amylase incorporated by LbL were used as samples. Furthermore the activity of LbL silicone samples was determined after 24 h washing in DI H_2O and after storage for 1 week.

5.4 LbL assembly on catheters

To coat the catheters the same procedure as in chapter 5.1 and 5.2.2 was repeated 10 times to obtain 9.5 bi-layers. The LbL build-up was done with acylase, amylase and alternating layers of both enzymes on untreated catheters.

5.4.5 Enzyme activity measurements

The activity of the enzymes on catheter was determined the same way as for LbL silicone samples, explained in chapter 5.3.4. The coated catheters were therefore cut in 2 cm long pieces. Different parts of the catheter were used to determine the activity: the head, the ribbed part and the smooth part (see figure 19).

Figure 19: Explanation of parts of catheters used for enzyme activity tests.
Different parts of catheters. The ribbed part forms the inflatable balloon.

5.4.6 Dynamic biofilm inhibition test

For the biofilm tests on catheters a dynamic system was developed (see figure 20). A bottle containing artificial urine pH 6.6 (for composition see table 8) was closed with a lid containing hoses and distributors. Then the whole system was autoclaved. Afterwards the artificial urine was inoculated with an ONC of

Pseudomonas aeruginosa to an OD_{600} of 0.01 and 4 catheters were added to the system (one Blank, one LbL acylase, one LbL amylase and one LbL with both enzymes).

Through a peristaltic pump the inoculated urine was pumped through each catheter with a velocity of 1 ml/min. The bottle containing the artificial urine was placed on a stirring plate and the solution was circulated with 100 rpm at room temperature. After 68 h the biofilm test was stopped and the catheters were removed from the setup.

Figure 20: Setup for dynamic biofilm test on catheters.

The bottle contains artifical urine that is inoculated with *P. aeruginosa*. This solution is pumped through the catheters with 1 ml/min to force the formation of biofilms.

Table 8: Composition of artificial urine

pH 6.6 in *[g/L DI H_2O] (according to standard "CSN EN 1616 - Sterile urethal catheters for single use")

Reagent	[g/L]*
Urea (CH_4N_2O)	25.0
Sodiumchloride (NaCl)	9.0
(Disodium hydrogen orthophosphate) Na_2HPO_4	2.5
Ammonium chloride (NH_4Cl)	3.0
Potassium dihydrogen orthophosphate (KH_2PO_4)	2.5
Creatinine ($C_4H_7N_3O$)	2.0
Sodium sulfite (Na2SO3)	3.0

After removing the catheters from the setup they were rinsed for 3 min (1 ml/min) with 0.9 % NaCl solution.

5.4.6.1 Bacterial adhesion assay

The heads of the catheters (see chapter 5.4.5) were cut and transferred into a sterile 15 ml tube containing 2 ml 0.9 % NaCl solution. Adherent bacteria were removed by sonication for 30 seconds and henceforth vortexing for 1 minute. The samples were serially diluted and plated on cetrimide agar plates. The plates were incubated at 37°C for 24 h.

5.4.6.2 Microscopy of catheters after biofilm test

For the other parts of the catheters the bacteria were methanol fixed by placing the samples for 2 min in absolute methanol. Then cross-sections were cut and the so produced rings were analysed using bright field microscopy.

IV. Results and Discussion

1. Enzyme characterisation

1.5 Protein content quantifications

The following graph (figure 21) shows the calibration curve for the BCA protein assay.

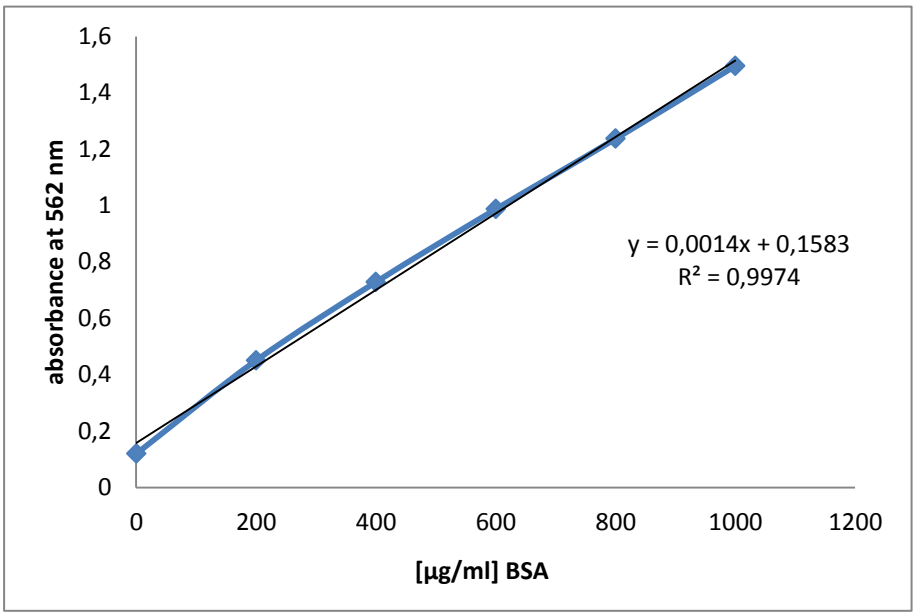

Figure 21: Standard curve of BCA protein assay.
BSA was used as a standard.

The equation of this standard curve (equation 3) was used for the determination of the enzymes' protein contents.

$$y = 0{,}0014x + 0{,}1583$$

Equation 3: Standard equation BCA protein assay

1.5.7 Acylase protein content

The protein content of the acylase powder was calculated using equation 3 and the absorbance values at 562 nm of the two acylase solutions with different concentrations of enzyme powder. An over-all average of all values was done and the protein content was calculated as 44 %. This means that 44 % of the powder is indeed protein (i.e. 1 mg/mL solution = 0.44 mg/mL protein).

1.5.8 Amylase protein content

The protein content of the amylase solution was calculated using equation 3 and the absorbance values at 562 nm of the two amylase solutions with different concentrations. An over-all average of all values was done and the protein content was calculated as 12.5 mg/ml protein.

1.6 Acylase activities

1.6.1 Standard curve with L-methionine

Figure 22 shows the calibration curve for acylase activity in solution with different concentrations of L-methionine as a standard.

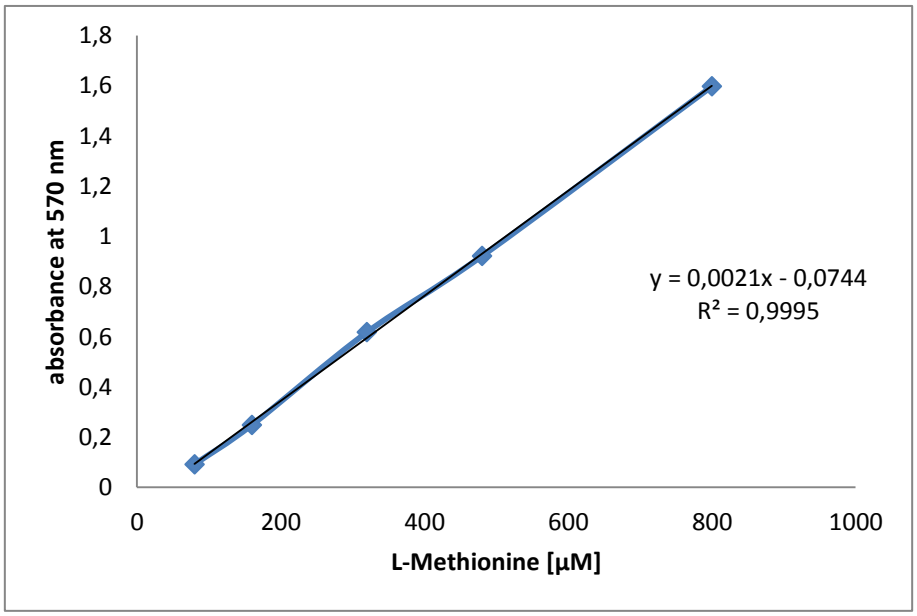

Figure 22: Standard curve for acylase activity in solution.
L-methionine was used as a standard.

The following equation (equation 4) was used to determine the enzymatic activity of acylase in solution.

$$y = 0{,}0021x - 0{,}0744$$

Equation 4: Standard equation for acylase activity in solution

1.6.2 Activity calculations for acylase

The following equations were used for all the enzyme activity calculations in solution.

The absorbance value at 570 nm of the blank was subtracted from the absorbance value of the test solution. This value was then used as "y" in equation 4.

$$x = \frac{(y + 0{,}0744)}{0{,}0021} = z\ \mu M\ L - methionine \quad \textbf{(5 A)}$$

$$enzyme\ activity = \frac{U}{ml} = \frac{\mu mol}{\min * ml} = \frac{z\ [\mu M]}{1000 * t\ [\min]} * df \quad \textbf{(5 B)}$$

$$\frac{U}{mg\ (solid)} = \frac{enzyme\ activity\ [\frac{U}{ml}]}{C\ [\frac{mg}{ml}]} \quad \textbf{(5 C)}$$

$$specific\ enzyme\ activity = \frac{U}{mg\ (protein)} = \frac{enzyme\ activity\ [\frac{U}{ml}]}{P\ [\frac{mg}{ml}]} \quad \textbf{(5 D)}$$

Equation 5: Calculation of enzymatic activity of acylase (5A- 5D)

The following table (table 9) shows the explanation of the abbreviations used in equation 5 and the usual volumes and concentrations used for this assay.

Table 9: Abbreviations and explanations of equation 5

Abbr.	Explanation	Volume/ Concentration
V_t	total enzyme reaction volume	0,5 [ml]
V_E	enzyme volume	0,1 [ml]
df	dilution factor of enzyme (V_t/V_E)	5
t	reaction time	30 min
C	acylase powder concentration	0,14 [mg/ml]
P	acylase protein concentration	44 % of C = 0,0616 [mg/ml]
z	liberated L-methionine in 30 min	[µM]

1.6.3 *Temperature- profile of acylase*

In figure 23 the specific enzyme activity [U/mg] is plotted against the assay temperature in [°C] which leads to the temperature- profile of acylase.

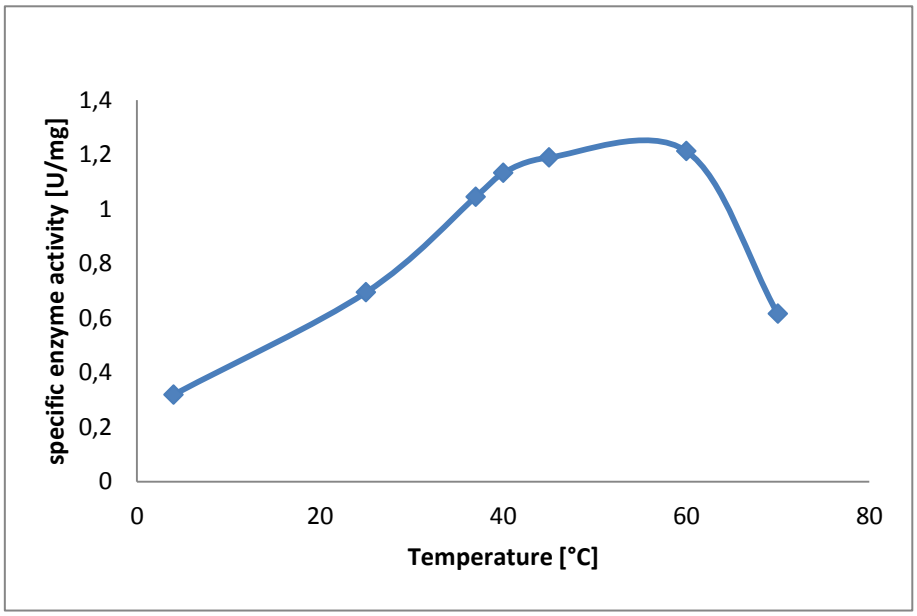

Figure 23: Temperature- profile of acylase.

The temperature optimum for acylase was determined as 40-50 °C. This corresponds to the information given from the supplier who claims the temperature optimum to be between 40-45°C. As the normal human body temperature is around 37 °C acylase will be active in this environment and usable for the application on catheters.

1.6.4 *pH- profile of acylase*

In figure 24 the specific enzyme activity [U/mg] is plotted against the pH values at which the enzyme assay was performed. This leads to the pH- profile of acylase.

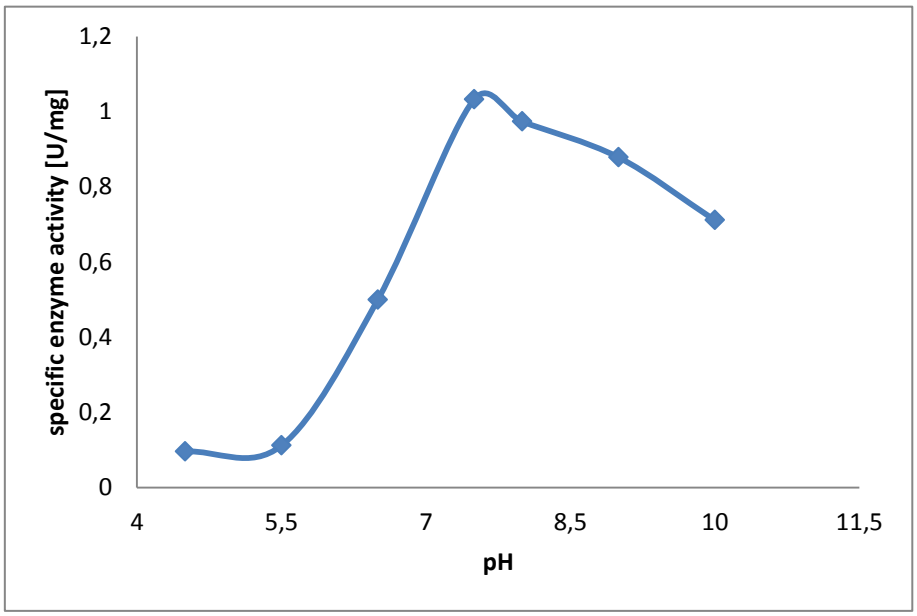

Figure 24: pH-profile of acylase

The pH-optimum for acylase is 8. The enzyme seems to be active at a pH range of 6-10. This correlates again with the values given by the supplier.

The pH of human urine can vary between 4.5 and 8, with a pH between 5 and 6 being normal [58]. *Proteus mirabilis* is a gram negative bacterium that has the ability to produce high levels of urease. Urease hydrolyses urea to ammonia and therefore makes the urine more alkaline. Catheter blockage by crystalline *Proteus mirabilis* biofilm is a common complication in patients undergoing long-term indwelling bladder catheterisation. In a study of Jones & co-workers the pH of the urine increased from 6.1 to about 8.6 due to a *Proteus mirabilis* infection [59].

The pH profile of acylase, with stability from a pH range of 6-10 and a pH optimum of 8 fits perfectly to the pH of urine and therefore for the application on catheters.

1.6.5 *Activity without $CoCl_2$ as a co-factor*

The assay performed without the addition of $CoCl_2$ solution as a cofactor showed, that acylase is still active without $CoCl_2$, but loses about 38 % of its activity.

1.6.6 *Michaelis Menten kinetics for acylase*

To calculate the Michaelis Menten kinetics the enzyme assay was performed with different substrate concentrations (see figure 25).

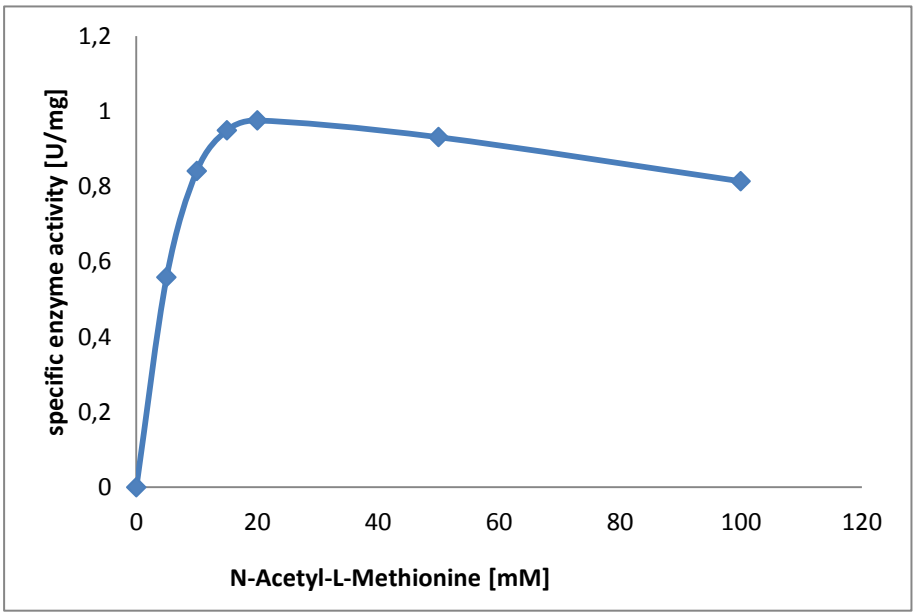

Figure 25: Acylase activity with different substrate concentrations for calculation of the Michaelis Menten kinetics.

The calculated values (using equation 2) are 1.3 U/mg for v_{max} and 6.64 mM for $K_{m.}$

1.7 Amylase activities

1.7.1 *Standard curve with maltose*

Figure 26 shows the calibration curve for amylase activity with different concentrations of maltose as a standard.

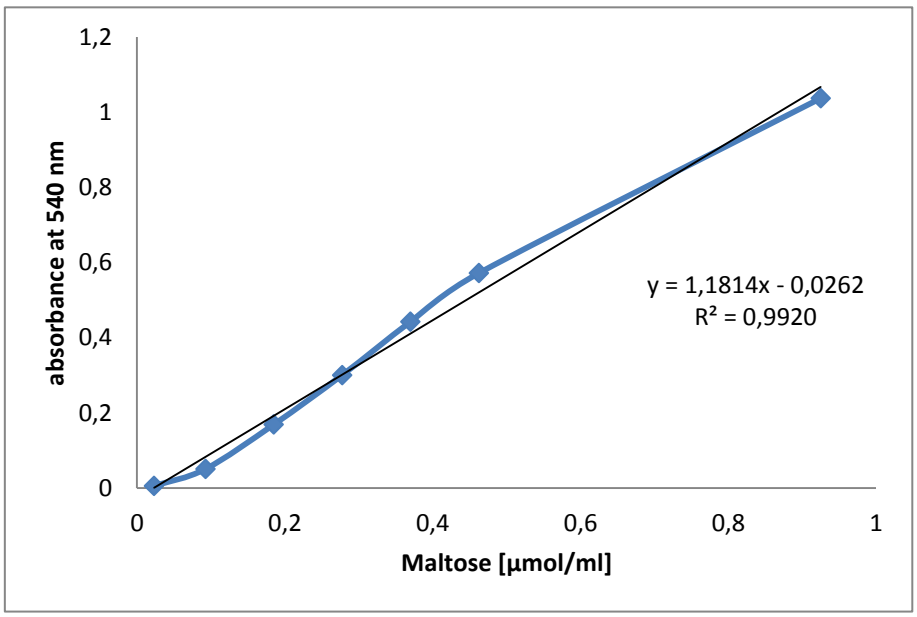

Figure 26: Standard curve for amylase activity.
Maltose was used as a standard.

$$y = 1{,}1814x - 0{,}0262$$

Equation 6: Standard equation for amylase activity.

Equation 6 was used to calculate the enzymatic activity of amylase.

1.7.2 Activity calculations for amylase

The following equations were used for all the enzyme activity calculations in solution.

The absorbance value at 540 nm of the blank was subtracted from the absorbance value of the test solution. This value was then used as “y” in equation 6.

$$x = \frac{(y + 0{,}0262)}{1{,}1814} = z\ \frac{\mu mol}{ml} maltose \quad \textbf{(7A)}$$

$$enzyme\ activity = \frac{U}{ml} = \frac{\mu mol}{\min * ml} = \frac{z\ [\mu mol/ml]}{t\ [\min]} * df \quad \textbf{(7 B)}$$

$$specific\ enzyme\ activity = \frac{U}{mg\ (protein)} = \frac{enzyme\ activity\ [\frac{U}{ml}]}{P\ [\frac{mg}{ml}]} \quad \textbf{(7 C)}$$

Equation 7: Calculation of enzymatic activity of amylase (7A- 7C).

The following table (table 10) shows the explanation of the abbreviations used in equation 7 and the usual volumes and concentrations used for this assay.

Table 10: Abbreviations and explanations of equation 7

Abbr.	Explanation	Volume/ Concentration
V_t	total enzyme reaction volume	1,2 [ml]
V_E	enzyme volume	0,05 [ml]
df	dilution factor of enzyme (V_t/V_E)	24
t	reaction time	3 min
P	amylase Protein concentration	[mg/ml]
z	liberated Maltose in 3 min	[µmol/ml]

1.7.3 *Temperature- profile of amylase*

In figure 27 the specific enzyme activity [U/mg] is plotted against the enzymatic assay temperature in [°C] which leads to the temperature- profile of amylase.

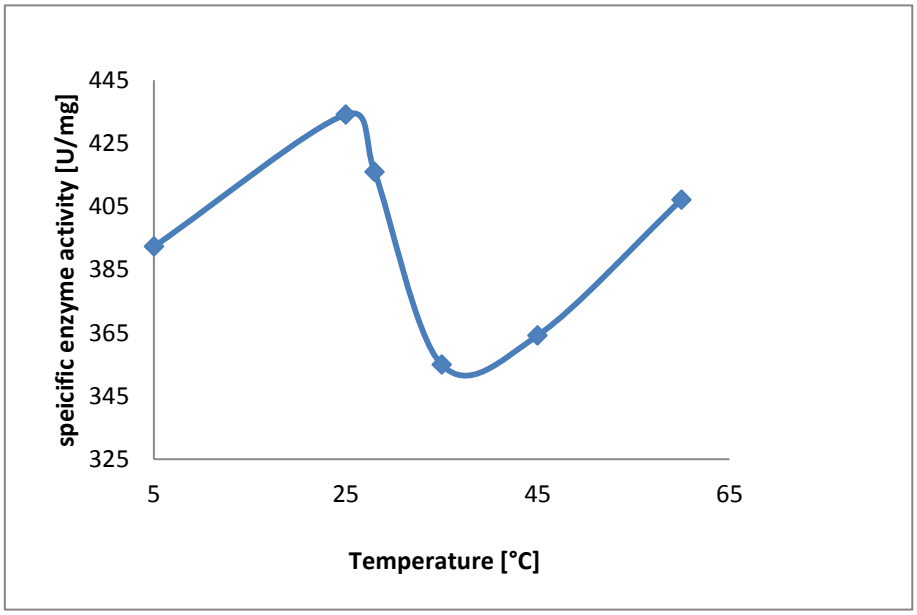

Figure 27: Temperature- profile of amylase.

The α-amylase from *Bacillus amyloliquefaciens* has two temperature optima. One is about 25°C and the other one starting at about 65°C. According to the supplier the enzyme is active at high temperatures (70-90°C).

The temperature profile of amylase does not fit appropriately for the application on the human body but the enzyme still shows activity at 37°C and the good stability on high temperatures can bring other advantages. Also, the immobilized enzyme is expected to be more stable.

1.7.4 pH- profile of amylase

In figure 28 the specific enzyme activity [U/mg] is plotted against the pH value of the assay which leads to the pH- profile of amylase.

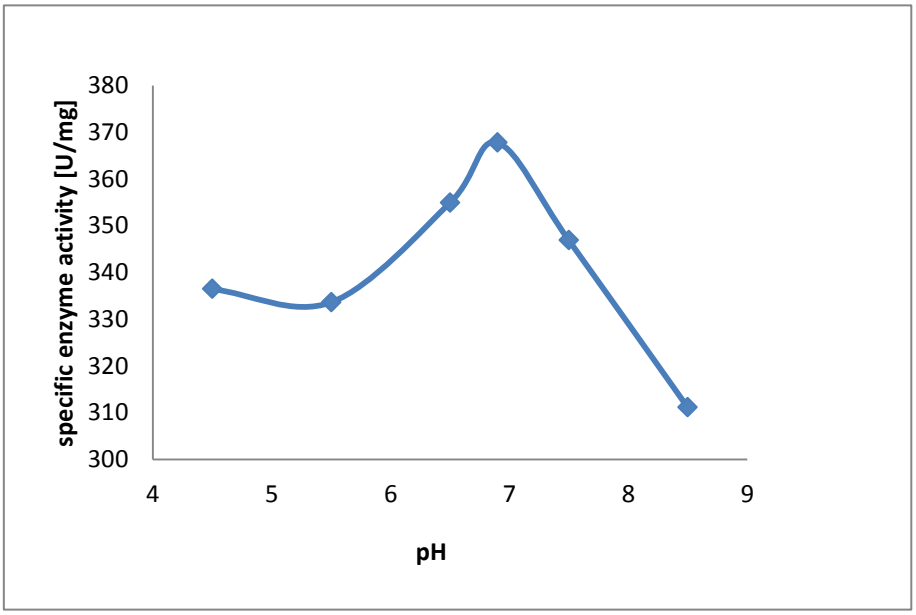

Figure 28: pH-profile of amylase.

The optimum pH of α-amylase is about 7, but the enzyme is stable at a pH range from around 4 to 7.5. At a pH higher than 7.5 the activity decreases rapidly.
Anyhow, also α-amylase should be able to work in the environment of human urine and can be used to coat catheters.

1.7.5 Michaelis Menten kinetics for amylase

To calculate the Michaelis Menten kinetics the enzyme assay was performed with different substrate concentrations.

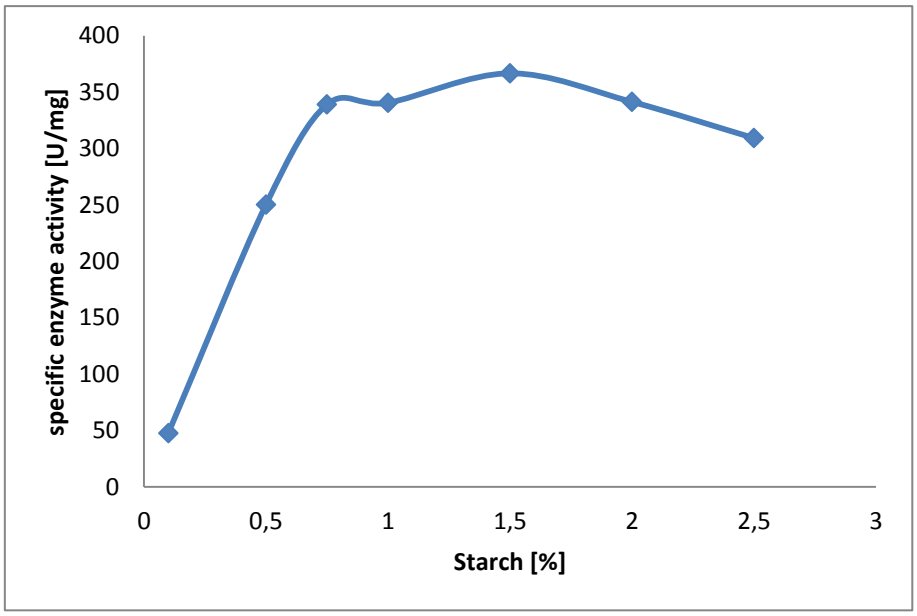

Figure 29: Amylase activity with different substrate concentrations for calculation of Michaelis Menten kinetics.

The calculated values (using equation 2) are 477.7 U/mg for v_{max} and 0.455 % for $K_{m.}$

1.8 Interference tests

The enzyme assays performed with a mixture of acylase and amylase showed that there is no interference on the activity of the two enzymes in solution. They neither boost nor decrease each other's activity.

2. Microtiter plate biofilm inhibition assay

To prove the ability of the chosen enzymes a microtiter plate biofilm inhibition assay with enzymes in solution was performed. Figure 30 shows some parts of a microtiter well plate during a biofilm inhibition assay with *P. aeruginosa*. The picture was taken after staining with crystal violet and before dissolving the stain with EtOH. The biofilm formation can be clearly seen at the controls and the negative controls (buffers). There is no biofilm visible at the wells that are treated with antibiotic, as well as at the blank wells. The wells treated with acylase or amylase also show almost no biofilm formation. For the explanation of figure 30 see table 11.

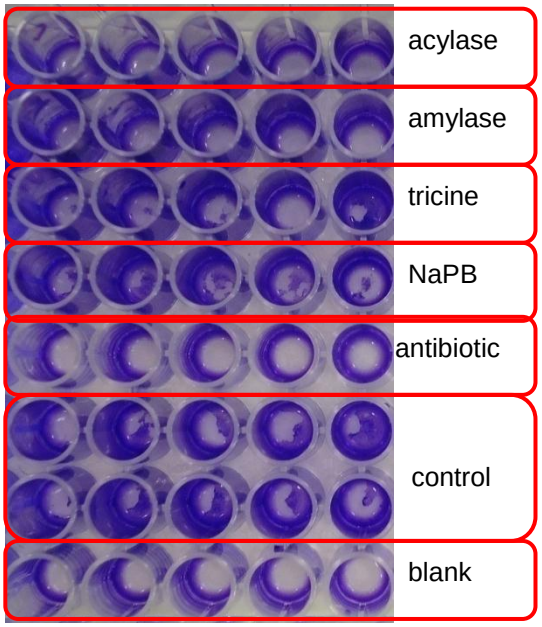

Figure 30: Microtiter wells from a biofilm inhibition test.

Biofilm inhibition test of acylase and amylase with *P. aeruginosa*. The picture was taken after staining with crystal violet, but before dissolving the dye in EtOH. The dark violet colour at the control wells, as well as at the tricine and NaPB treated samples shows the biofilm formation. The blanks and the wells with antibiotics don't show a colour. The samples treated with acylase or amylase show almost no colour, which means no biofilm formation.

Table 11: Explanation for figure 30

Solution	Explanation
Acylase	15 µl of 0,2 U/ml acylase added to 135 µl bacterial suspension
Amylase	15 µl of 5,7 U/ml amylase added to 135 µl bacterial suspension
Tricine	15 µl of 100 mM tricine buffer pH 8 added to 135 µl bacterial suspension
NaPB	15 µl of 20 mM sodiumphosphate buffer with 6,7 mM NaCl pH 6,9 added to 135 µl bacterial suspension
Antibiotic	15 µl of 100 µg/ml gentamicin added to 135 µl bacterial suspension
Control	150 µl of bacterial suspension
Blank	150 µl of sterile MH broth

The average absorbance value of the blanks at 540 nm was subtracted from the OD_{540} average value of the different samples. The control without any additive was set 100 % and the biofilm inhibition of all solutions was calculated in relation to the control.

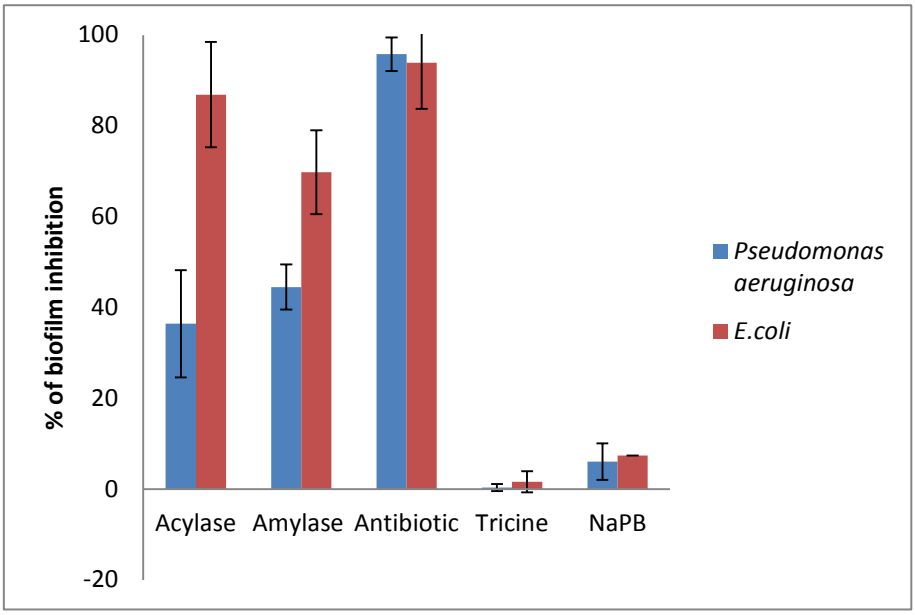

Figure 31: Microtiter plate biofilm inhibition.

Both enzymes showed biofilm inhibiton on *P. aeruginosa* and *E. coli*. The antibiotic was added as a positive control, to confirm that the assay works. The buffers were used as negative controls, to proof that the used buffers are not the reaseon fot the bioiflm inhibition caused by the enzymes.

acylase 0.2 [U/ml]; amylase 5.7 [U/ml]; antibiotic 100 [µg/ml]; 100 mM tricine buffer pH 8; 20 mM sodiumphosphate buffer with 6.7 mM NaCl pH 6.9

Both enzymes showed biofilm inhibition on *P. aeruginosa* and *E. coli*. There is no biofilm formation detectable for the samples where antibiotic was added. The inhibition was at almost 100%, which proves that the principle of the assay works. The buffers used for the enzymes don't show a relevant biofilm inhibition.

It is not clear, why there is such a great effect of acylase on *E. coli* as it is reported in the literature that *E. coli* does not produce AHLs (as already mentioned before). However, we found that acylase is able to decrease the biofilm formation of *E. coli*. Other mechanisms rather than degradation of AHLs might be happening. Studies are ongoing to try to understand this issue.

Some improvements of the principle method could lead to more accurate results with smaller error bars. For example another broth that forces the biofilm formation, e.g. tryptic soy broth, could be used. Another possibility could be to fix the biofilm before staining by heat.

Anyhow, both enzymes showed inhibition of biofilm formation.

3. Silicone pretreatmens: Silanization with APTES

The silanization of the silicone with APTES was proven with a ninhydrin colour test. Untreated silicone serves as a blank and showed no colour development. The APTES treated silicone showed dark purple colour (see figure 32).

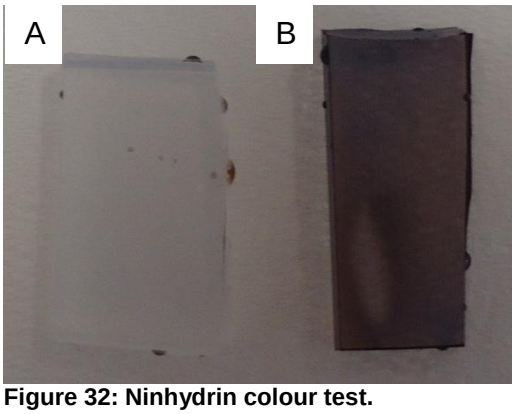

Figure 32: Ninhydrin colour test.
A: Blank with no colour development, B: APTES silicone got coloured

4. LbL approaches

4.1 Fluorescence microscopy of FITC labelled enzymes

To prove the film assembly and to compare the basic structure of the multilayer film a Lbl build-up with FITC-labelled enzymes on silicone and on APTES silicone was performed.

The following fluorescence microscopy pictures show the structure of the LbL assembly on silicone and on APTES silicone with these FITC-labelled enzymes. Figure 33 and figure 34 show the LbL assemblies of FITC- labelled acylase and FITC- labelled amylase on silicone. In figure 33 picture A and B are focused on different layers. But also for amylase the different enzyme layers on the silicone are clearly visible.

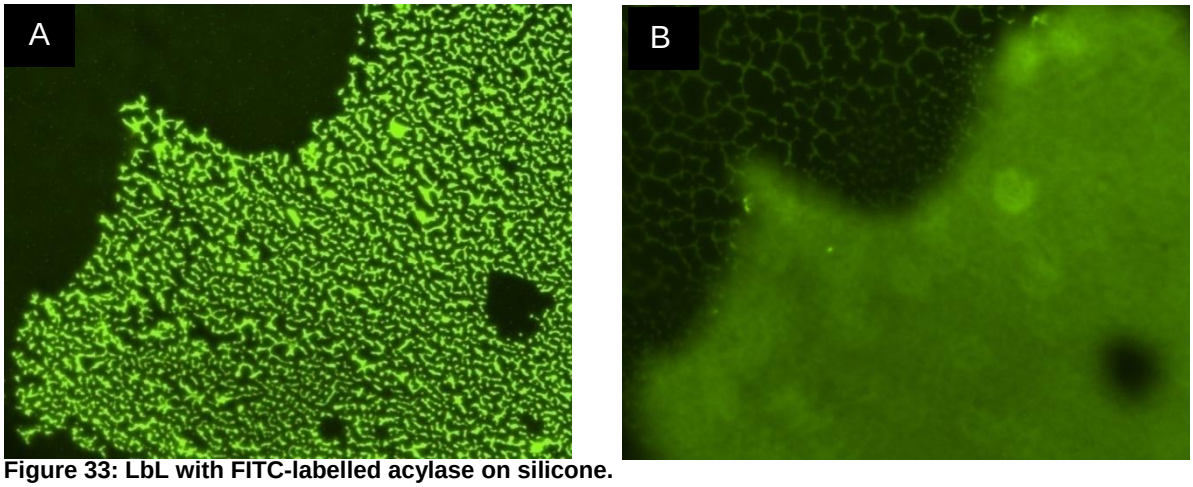

Figure 33: LbL with FITC-labelled acylase on silicone.

4.5 bilayers with labelled acylase were built up on silicone. The different layers are clearly visible, as picture A and B are focused on different layers. Magnification: x 100; Exposure time: 1 sec

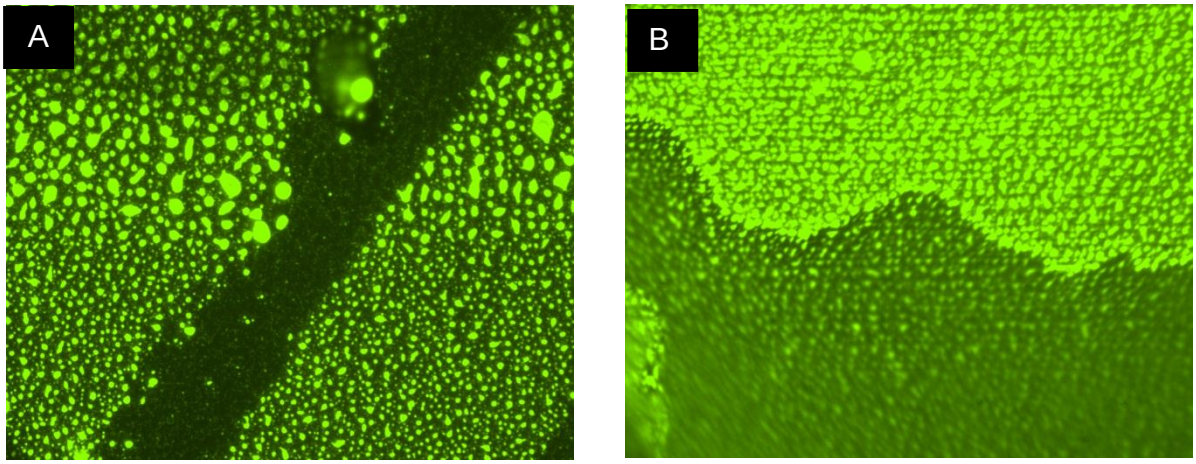

Figure 34: LbL with FITC-labelled amylase on silicone.

4.5 bilayers with labelled amylase were built up on silicone. The different layers are clearly visible, especially in picture B. Magnification: x 100; Exposure time: 426 ms

In figure 35 and figure 36 the LbL assemblies of FITC- labelled acylase and FITC-labelled amylase on APTES silicone are visible. Here the layers seem more homogenous and therefore the different layers are not as clearly visible as for silicone without APTES. Especially the amylase layers appear very cross-linked. This tightness might bring the problem of steric hindrance with it and could therefore decrease the enzyme's activity.

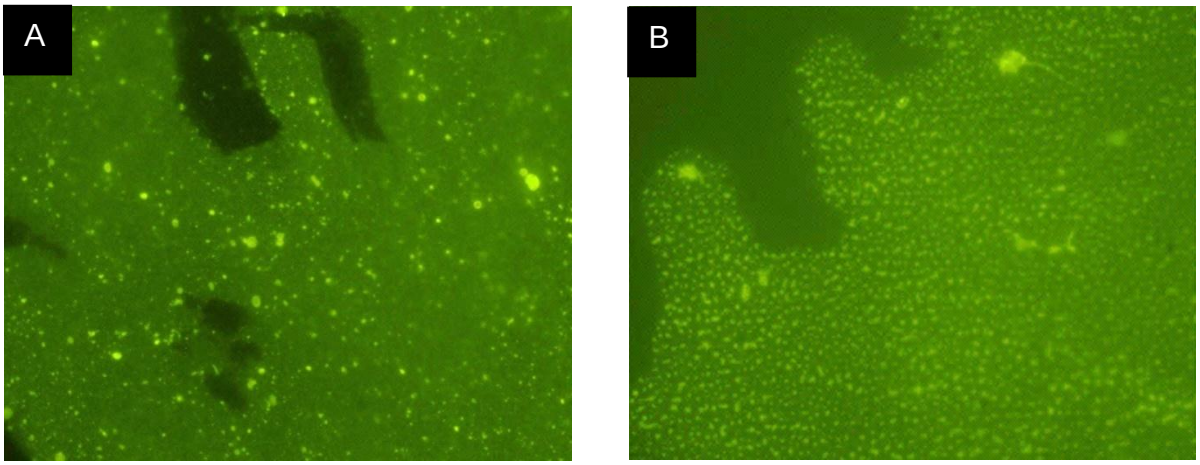

Figure 35: LbLwith FITC-labelled acylase on APTES silicone.

4.5 bilayers with labelled acylase were built up on APTES silicone. The layers on APTES silicone appear more homogenous compared to the ones on untreated silicone. Magnification: x 100; Exposure time: 1 sec

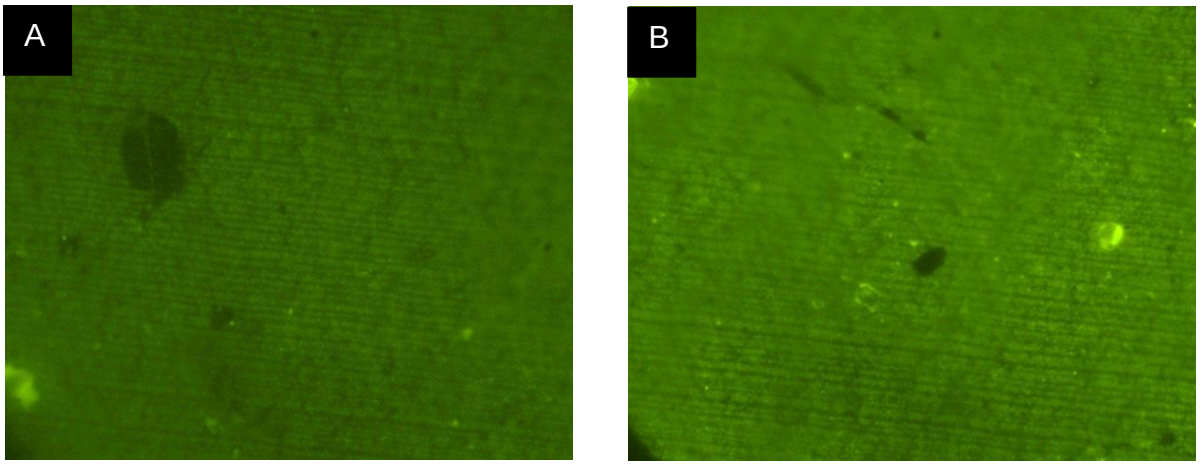

Figure 36: LbL with FITC-labelled amylase on APTES silicone.

4.5 bilayers with labelled amylase were built up on APTES silicone. The layers seem to be very tight and the different layers are not clearly visible. Magnification: x 100; Exposure time: 426 ms

Figure 37 shows the LbL assembly of FITC- labelled amylase on silicone and APTES silicone with 10 x magnifications. The scratches were produced on purpose to make clear that everything that is fluorescent is really labelled enzyme.

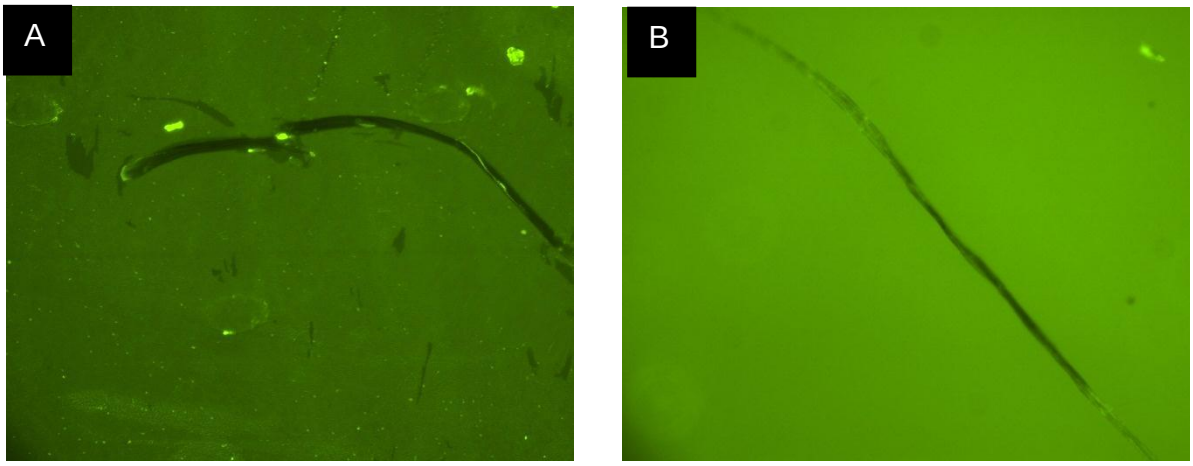

Figure 37: A: LbL with FITC-labelled amylase on silicone. B: LbL with FITC-labelled amylase on APTES silicone

4.5 bilayers with labelled amylase were built up on silicone and APTES silicone. The fluorescence is much higher when the silicone was pre-treated with APTES. The scratches were produced on purpose to make sure, that everything that is fluorescent is really labelled enzyme. Magnification x 10; Exposure time: 426 ms

4.2 FTIR

4.2.1 LbL samples vs. LbL APTES samples

The FTIR technique was used to obtain an infrared spectrum of absorption.

The following figures show FTIR spectra (analysed with the software eFTIR) of LbL samples and LbL APTES samples. To prove that the multilayer film is stable, also the FTIR spectra of the washed samples are shown.

Figure 38 and figure 39 show the whole FTIR spectrum of all samples on silicone and APTES silicone. The highlighted parts (red circles) can be seen in higher magnification again in the next graphs.

Figure 38 shows clearly that at the highlighted wavenumbers new peaks are appearing that are not there at the blanks.

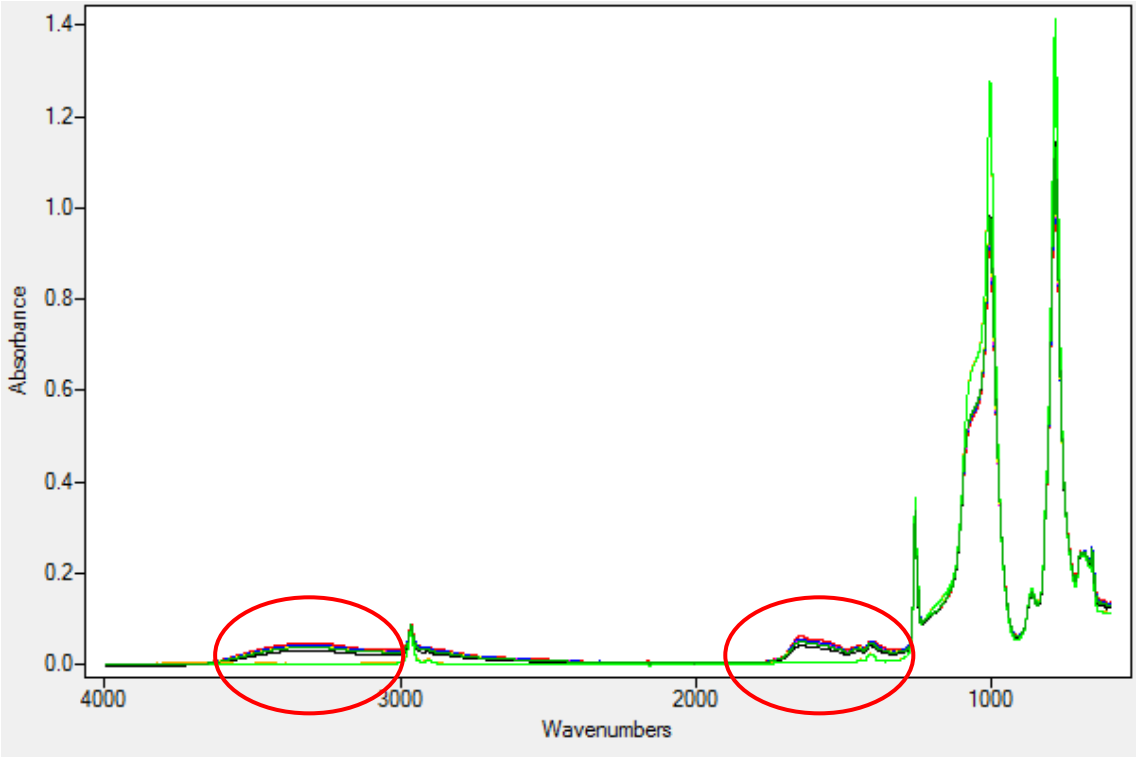

Figure 38: FTIR spectra of LbL samples.

LbL samples and LbL samples after washing 24h in H_2O.

The highlighted parts (red circles) show where there are differences between the blank and the samples, these parts are shown again in figure 41 and figure 44.

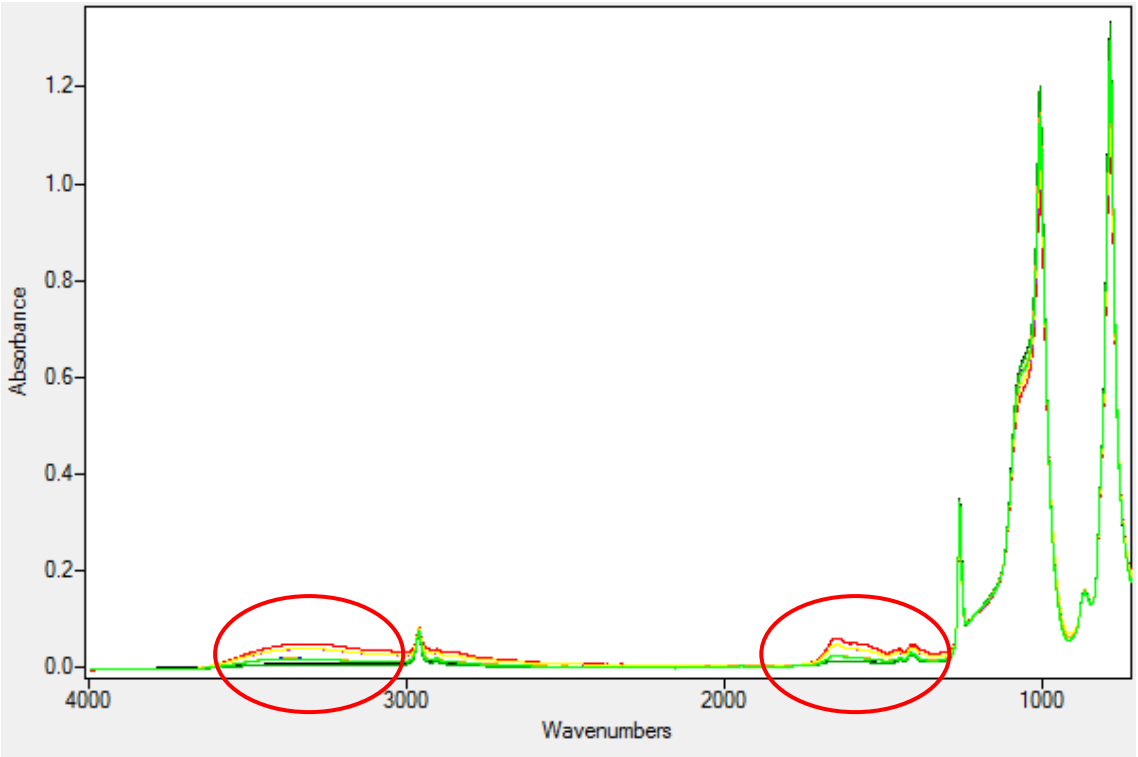

Figure 39: FTIR spectra of LbL APTES samples.

LbL samples and LbL APTES samples after washing 24h in H_2O.

The highlighted parts (red circles) show where there are differences between the blank and the samples, these parts are shown again in figure 42 and figure 45.

Hydrogen bonding plays an important role in the determination of the three-dimensional structure of proteins. Bonds within the same macromolecule are the reason for folding into a specific shape. In the secondary structure of proteins, hydrogen bonds form between the backbone oxygen and amide

hydrogen [60; 54; 61].

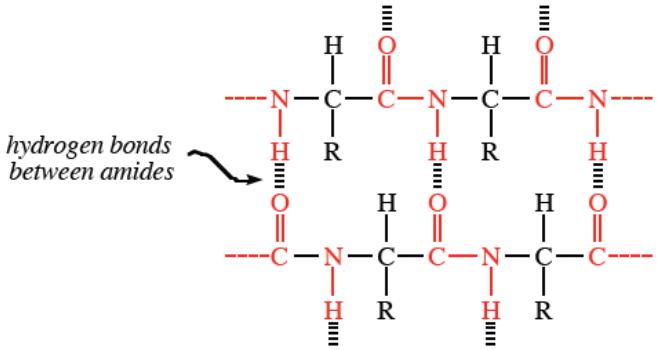

Figure 40: The hydrogen bonds [61].

formed between amide bonds buried inside a folded protein

So the peaks at the wavenumber 3350 [cm^{-1}] could be assigned to hydrogen bonding due to OH-groups, a typical functional group present in proteins.

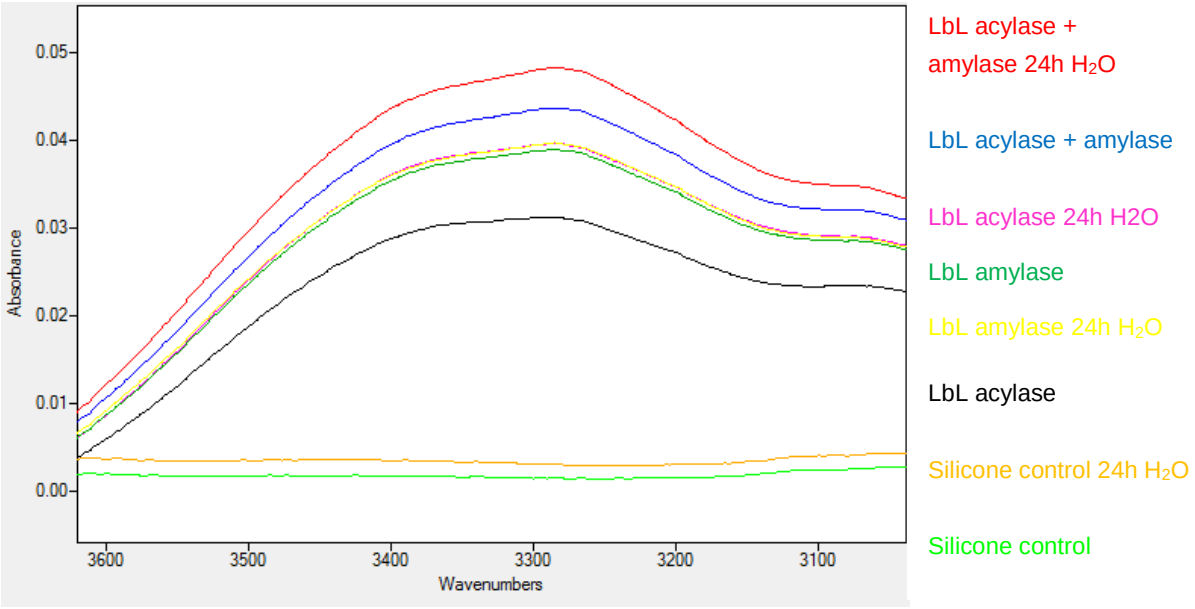

Figure 41: FTIR spectra (at 3600- 3100 [cm^{-1}]).

LbL samples and LbL samples after washing 24h in H_2O. The peak that appears at the samples compared to the controls could be assigned to hydrogen binding due to the OH-groups (3350 [cm^{-1}]). The peak is not disappearing after washing.

There is a clear difference between the blanks and the samples visible.

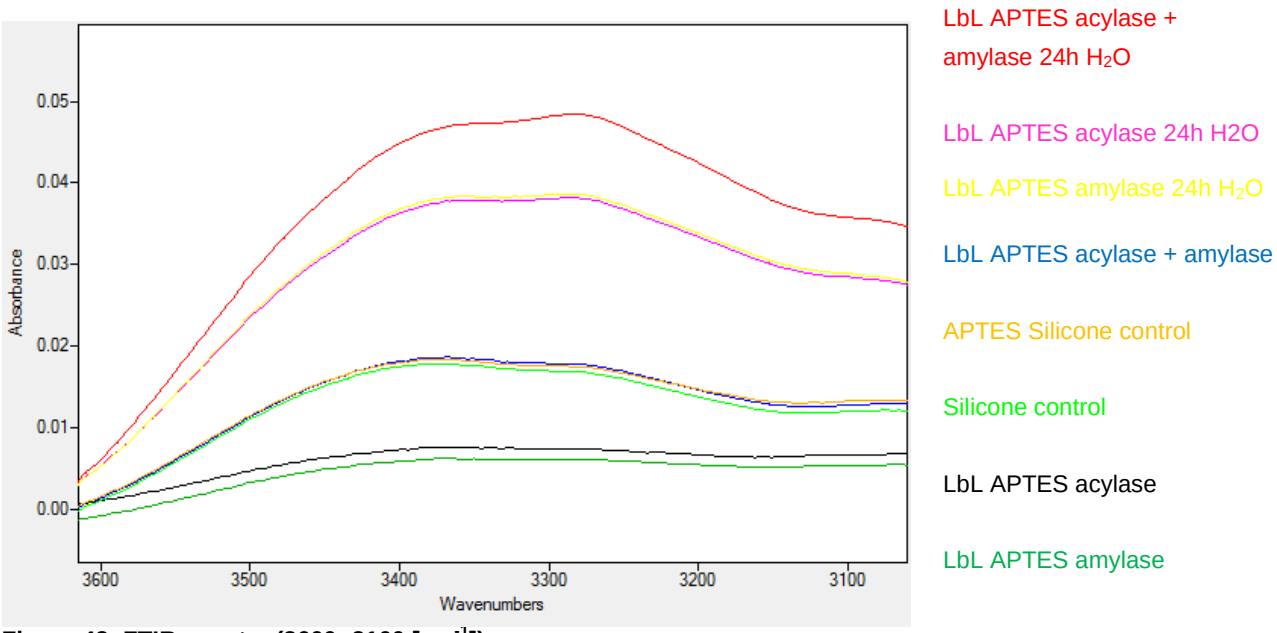

Figure 42: FTIR spectra (3600- 3100 [cm^{-1}])

LbL APTES samples and LbL APTES samples after washing 24h in H_2O. The peak that appears at the samples compared to the controls could be assigned to hydrogen binding due to the OH-groups (3350 [cm^{-1}]). The peak is not disappearing after washing.

The peak at the wavenumber 1650 [cm^{-1}] corresponds to the amide I band. Proteins are chains of amino acids held together by peptide bonds (i.e. amide bonds). This leads to the assumption that the protein is really bound on the surface.

The following figure shows the vibration that is responsible for the amide I band in the infrared spectra of proteins. The amide I band appears due to the carbonyl stretching vibrations [61].

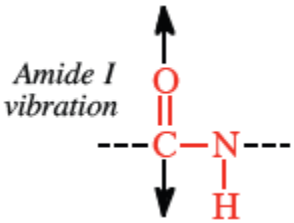

Figure 43: Carbonyl stretching vibration responsible for Amide I band [61].

For the silicone samples the amide I band only appears at the LbL samples. For the APTES silicone samples this is not that clear, because also the blanks show a small peak.

Anyhow the amide I band does not disappear after a 24h washing step in water. This is a proof of the stability of the established multilayer films.

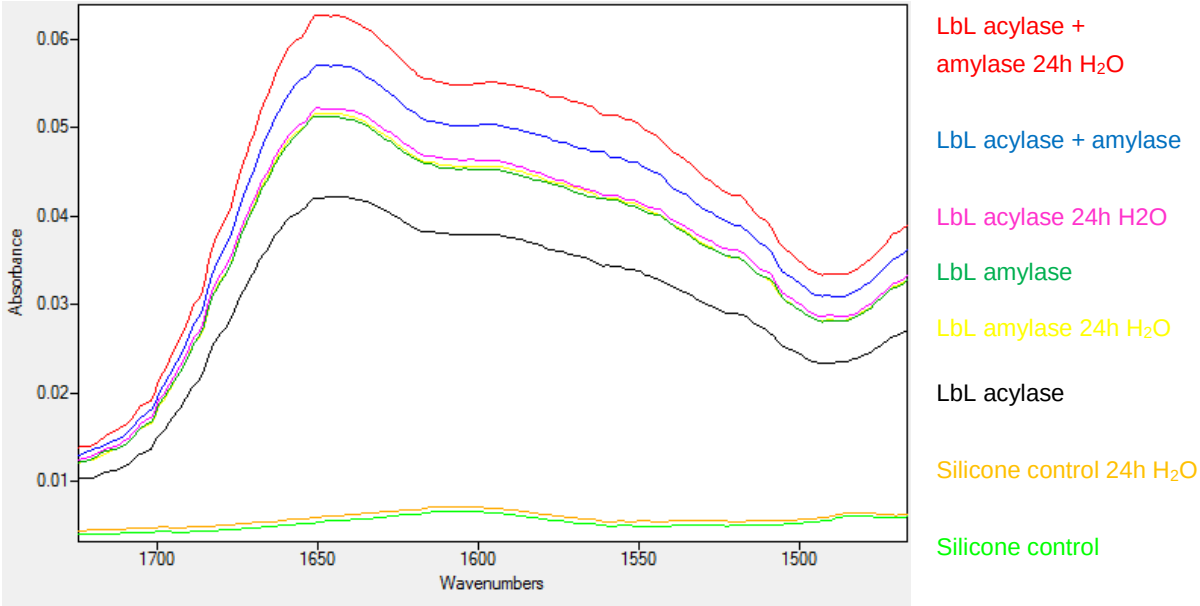

Figure 44: FTIR spectra (1700- 1500 [cm^{-1}]).

LbL samples and LbL samples after washing 24h in H_2O. The appearing amide I band (1650 [cm^{-1}]) leads to the assumption that the protein is really bound on the surface. After washing, the band does not disappear.

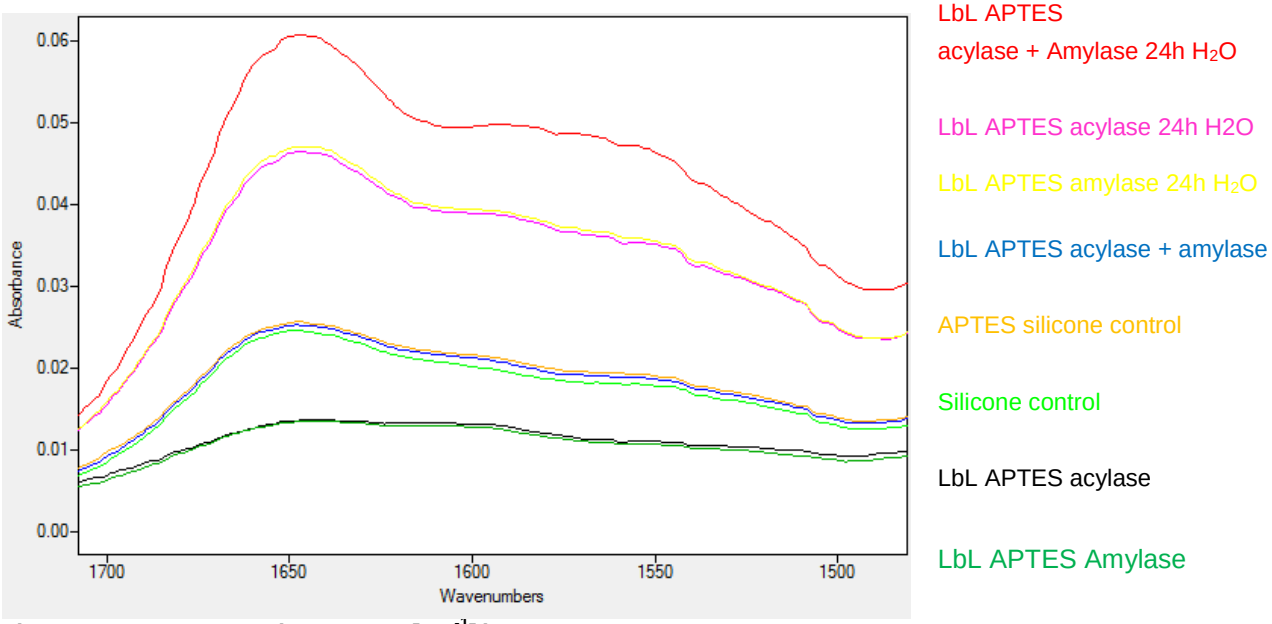

Figure 45: FTIR spectra (1700- 1500 [cm^{-1}]).

LbL APTES samples and LbL APTES samples after washing 24h in H_2O. The appearing amide I band (1650 [cm^{-1}]) leads to the assumption that the protein is really bound on the surface. The band does not disappear after washing.

The FTIR spectra are a proof for the successful attachment of the enzymes and also for the stability of this attachment.

4.3 Water contact angle

The surface wettability of multilayer films was investigated. Figure 46 shows pictures from the water contact angle measurement on LbL silicones and figure 47 shows the average values of the contact angle. The water contact angle of all samples is decreased in comparison to the control silicone, which means that all LbL samples are more hydrophilic than the control. Especially the LbL film that only contains acylase leads to a really hydrophilic surface. The hydrophilicity of the samples is maintained after a 24h washing step in water.

This leads to the assumption that the multilayer film was successfully established and the film cannot be washed away easily in water.

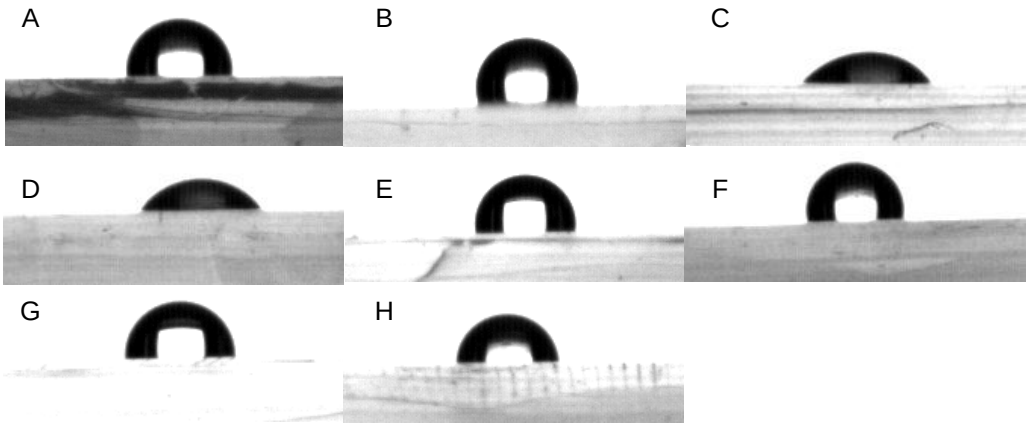

Figure 46: Water contact angle of LbL samples.

All samples appear more hydrophilic compared to the controls. The most hydrophilic one is the LbL assembly with only acylase. For all samples the hydrophilicity is maintained after a washing step.

A= Silicone control; B= silicone control 24h washed; C= LbL acylse; D= LbL acylase 24h washed; E= LbL amylase; F= LbL amylase 24h washed; G= LbL acylase + amylase; H= LbL acylase+ amylase 24h washed

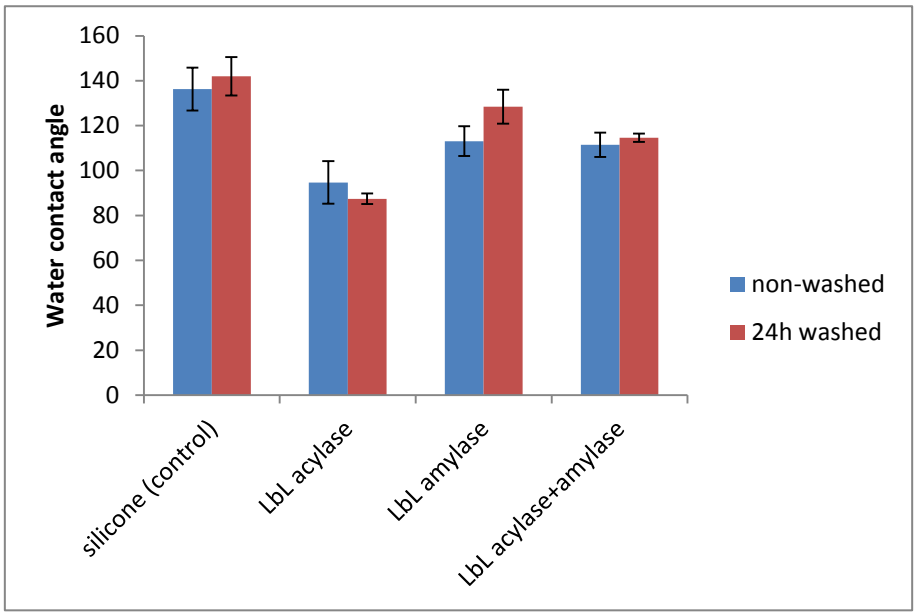

Figure 47: Water contact angle of LbL samples.

The water contact angle decreases due to the bound protein. Especially the samples with only acylase appear more hydrophilic. The hydrophilicity is maintained after a 24 h washing step.

A major problem in biomedical implants is biofouling, an undesired attachment of biomacromolecules (e.g. proteins) or organisms. The adsorption of proteins onto a surface is a complex process and not yet investigated entirely. Anyhow, adsorption can be discussed as two limiting mechanisms, electrostatic interactions and hydrophobic interactions. At the moment only few materials are known to effectively resist protein adsorption from biological fluids including poly(ethylene glycol) (PEG), oligo(ethylene glycol) (OEG) self-assembled monolayers (SAMs), zwitter-ionic materials and various hydrophilic biomacromolecules (e.g. dextran) [62].

This suggests that the increased hydrophilicity of the silicone surface due to the enzyme attachment could inhibit the adsorption of proteins.

4.4 SEM

To attempt the visualisation of the multi-layered surface morphology, SEM pictures of the silicone (control) and the silicone with LbL of acylase (9.5 bilayers) were taken. Figure 48 shows the SEM pictures of the silicone blank at different magnifications. The surface was found to be smooth.

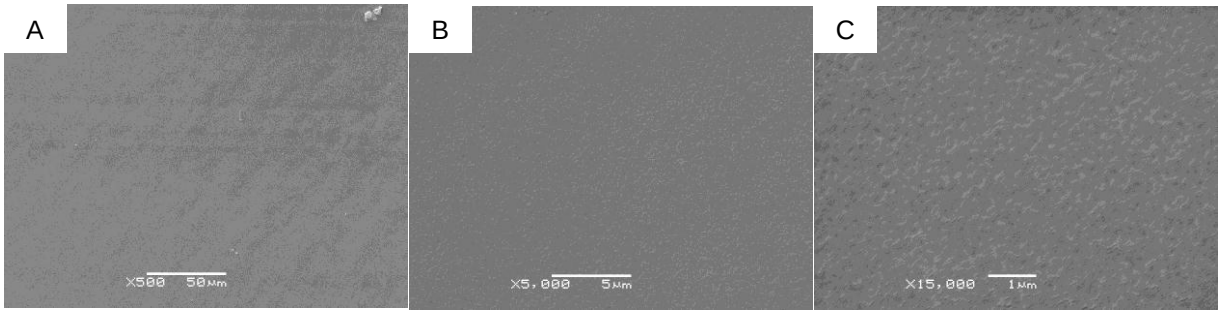

Figure 48: SEM pictures of silicone blank.
The untreated silicone surface was found to be smooth. A= x500; B=x5000; C=x15 000

In figure 49 the SEM pictures of a LbL acylase sample are shown. On picture A the salt from the washing solution is visible. In the background of picture A and on pictures B and C the different layers of the film are clearly visible.

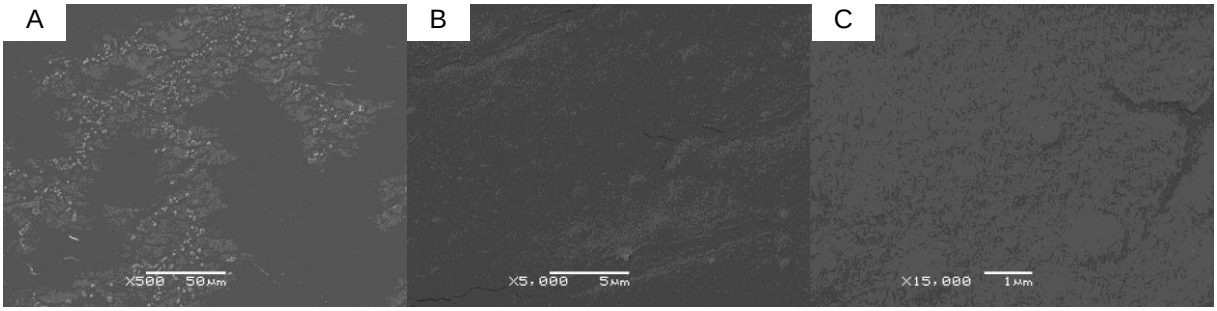

Figure 49: SEM pictures of LbL Acylase silicone 9.5 bilayers.
On Picture A the salt from the washing solution is visible. Pictures B and C show the different enzyme layers. The surface is not that smooth anymore. A= x500; B= x5000; C= x15 000

4.5 Enzyme activities

4.5.2 Acylase activity

4.5.2.1 Standard curve with L-methionine

Figure 50 shows the calibration curve of the acylase activity with different concentrations of L-methionine as a standard that was done for LbL conditions.

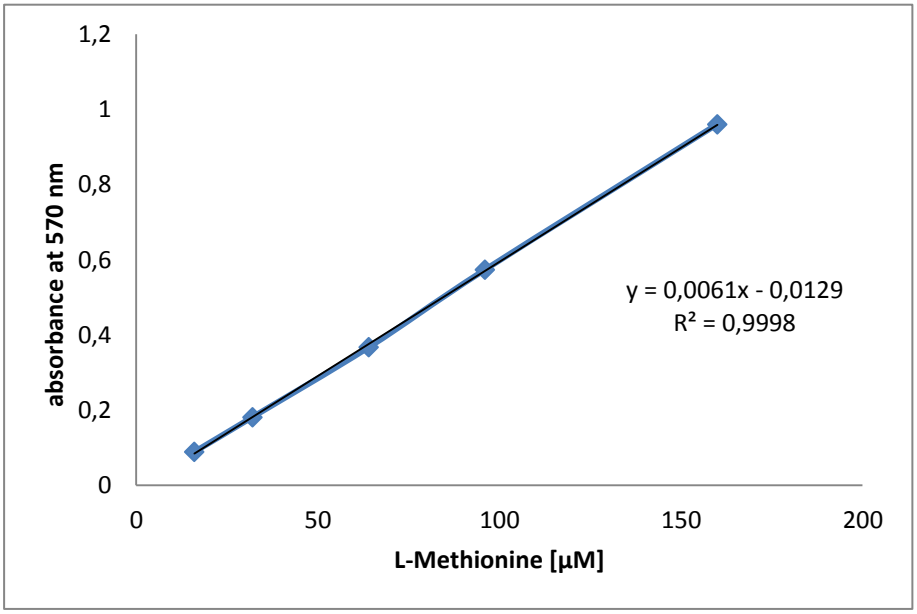

Figure 50: Standard curve for acylase activity on LbL.
L-methionine was used as a standard

The following equation (equation 8) was used to determine the enzymatic activity of acylase on LbL silicone.

$$y = 0{,}0061x - 0{,}0129$$

Equation 8: Standard equation for acylase Activity on LbL silicone

4.5.2.2 Activity measurements on LbL silicone

The following graphs (figure 51 and figure 52) show the enzymatic activity of acylase when incorporated on silicone in a LbL-fashion. The values were calculated using equation 8 and referenced to the silicone weight. The activity was measured immediately after the LbL build-up, after storage for 1 week at room temperature and after 24 h washing in DI H_2O at 37°C.

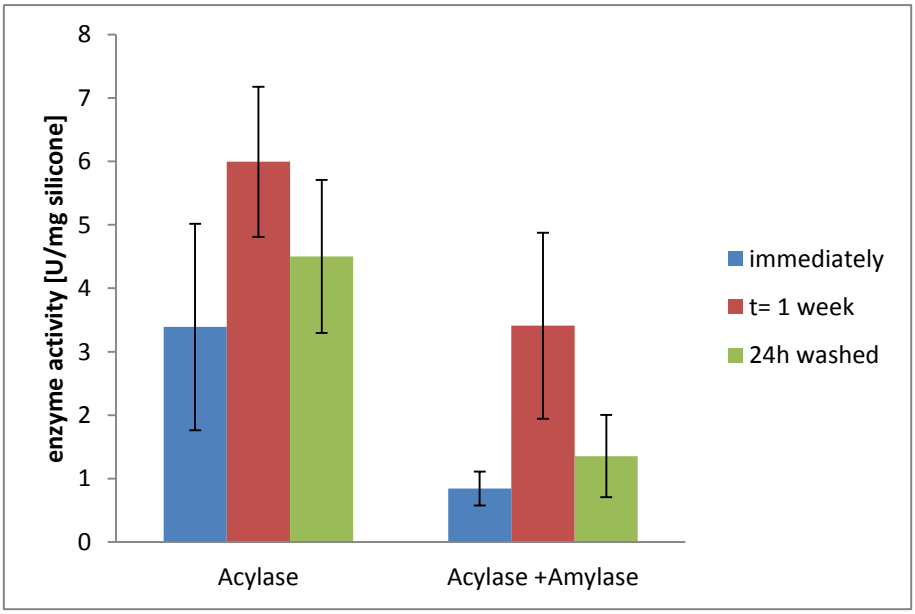

Figure 51: Acylase activity in [U/mg silicone] on LbL silicone.

The enzymatic activity of acylase when incorporated into the LbL assembly on silicone was determined at three different conditions: immediately after preparing, after 1 week of storage at room temperature and after a 24h washing step. Acylase was found to be active, even after storage and washing. Acylase= LbL with only acylase; acylase + amylase= LbL with both enzymes alternately, last layer here is amylase

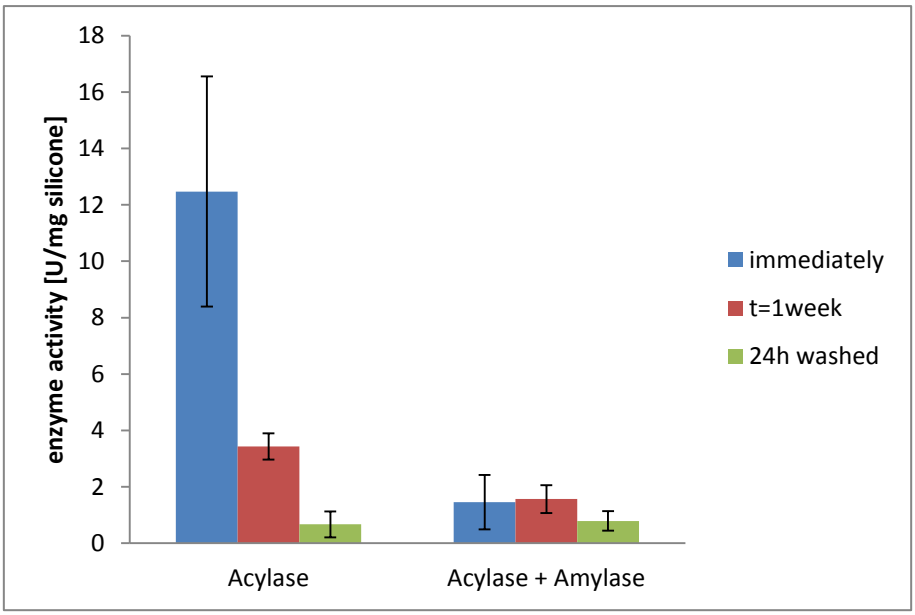

Figure 52: Acylase activity in [U/mg silicone] on LbL APTES silicone.

The enzymatic activity of acylase when incorporated into the LbL assembly on APTES silicone was determined at three different conditions: immediately after preparing, after 1 week of storage at room temperature and after a 24h washing step. Acylase was found to be active, but there was a big activity loss detectable after storage and washing. Acylase= LbL with only acylase; acylase + amylase= LbL with both enzymes alternately, last layer here is amylase

Although at first acylase seems to be more active on APTES silicone, the LbL assembly on silicone without APTES seems more stable. The loss of activity after

washing and storage is much higher on APTES silicone then on not-functionalised silicone. The enzymatic activity of acylase together with amylase is lower than only acylase, because the last layer was always amylase.

4.5.3 *Amylase activity*

Figure 53 shows the enzymatic activity of amylase when incorporated on silicone in a LbL-fashion. The values were calculated using equation 6 and referenced to the silicone weight. The activity was measured immediately after the LbL build-up, after storage for 1 week at room temperature and after 24 h washing in DI H_2O at 37°C.

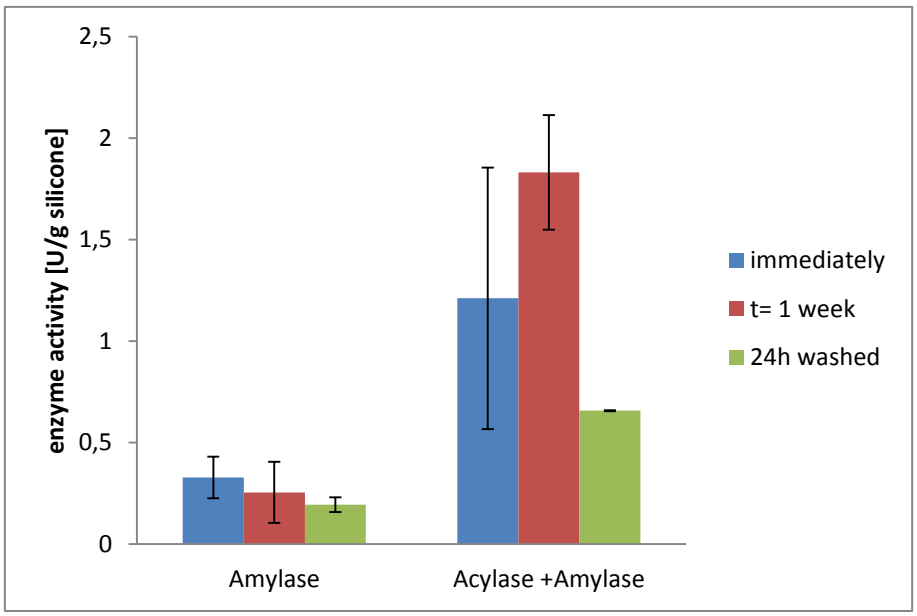

Figure 53: Amylase activity in [U/g silicone] on LbL silicone.

The enzymatic activity of amylase when incorporated into the LbL assembly on silicone was determined at three different conditions: immediately after preparing, after 1 week of storage at room temperature and after a 24h washing step. Amylase was found to be active, even after storage and washing although the determined activity was much higher when the LbL assembly was performed with both enzymes. amylase= LbL with only amylase; acylase + amylase= LbL with both enzymes alternately, last layer here is amylase

There was no enzymatic activity detectable on APTES silicone.

On silicone without functionalisation amylase shows much higher activity when incorporated alternated with acylase. As there is no such interference when both enzymes are in solution it could be that if only amylase is applied on the silicone the layers are too close to each other in such a manner that the enzyme cannot act. So the steric hindrance may be a reason for the inactive enzyme on APTES silicone. The experiments with FITC- labelled enzymes showed that the LbL build-up is tighter on APTES silicone than on silicone without treatment. So maybe there is more

enzyme on the surface after functionalisation with APTES, but therefore the active centre of the enzyme may be blocked. Also in solution amylase shows higher activity at lower concentrations.

But both enzymes showed activity when incorporated into a LbL film on silicone without pre-treatment and the activity could be maintained after storage for 1 week and a 24h washing step.

According to all these results the further LbL assemblies on catheters were performed without prior APTES functionalisation.

5. LbL assembly on catheters

The LbL approach was performed on silicone catheters. Figure 54 shows the catheters after LbL assembly. By the film deposition the catheters got coloured.

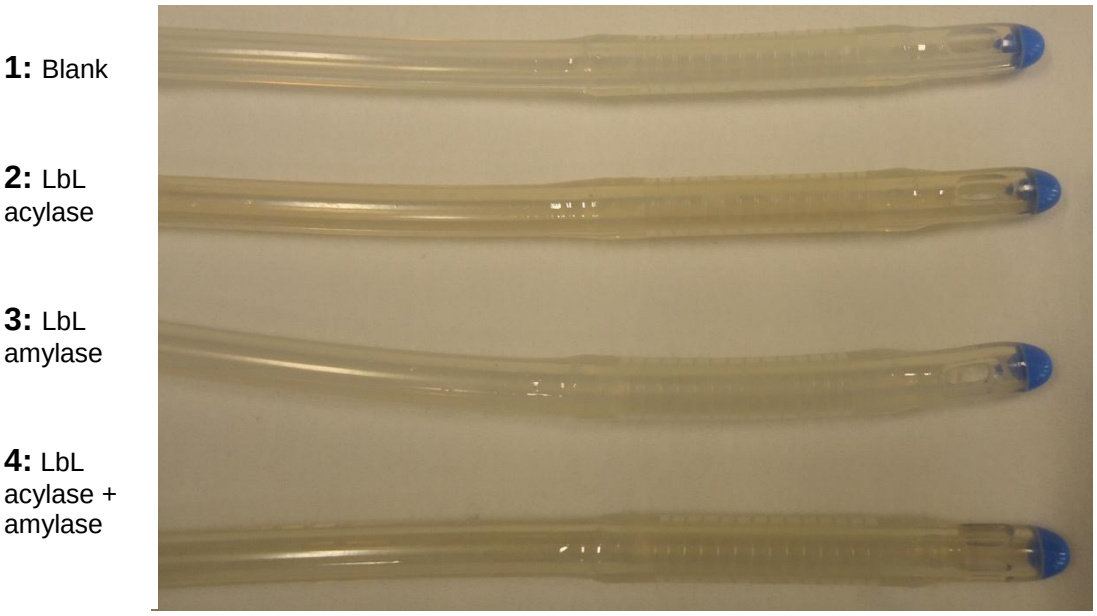

Figure 54: Catheters after LbL treatment.

The catheters get coloured by the film deposition. 1= Blank, untreated catheter; 2= LbL with acylase; 3= LbL with amylase, 4= LbL with acylase + amylase

5.1 Enzyme activities

The enzymatic activity of acylase on catheters could be determined. Figure 55 shows two cuvettes containing the colour reaction from the acylase activity assay. There is a clear difference between the blank and the sample.

Figure 55: Cuvettes from acylase activity test.
Colour difference between the blank and the sample is clearly visible.
1= blank solution; 2= LbL acylase catheter sample

Also the enzymatic activity of amylase on catheters could be determined. Figure 56 shows three cuvettes containing the colour reaction from the amylase activity assay. There is a clear difference in the colour visible between the blank and the samples.

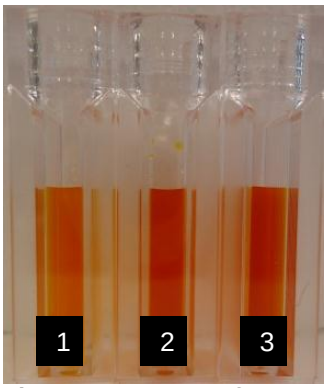

Figure 56: Cuvettes from amylase activity test.
Colour difference between the blank and the samples is clearly visible.
1= blank solution; 2= LbL amylase catheter sample;
3= LbL acylase+ amylase catheter sample

Figure 57 shows the enzymatic activity of acylase on catheters. The ribbed part of the catheter seems to be the most active one.

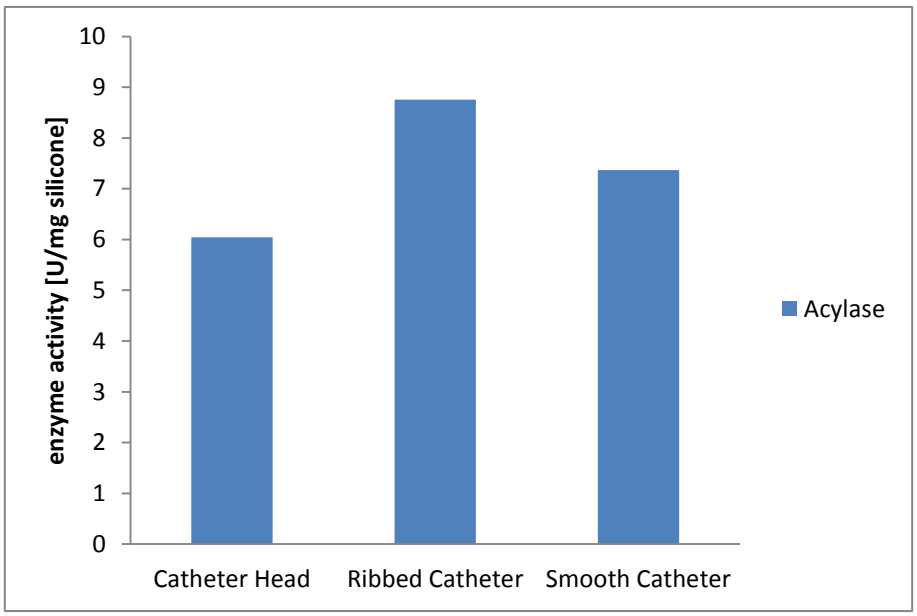

Figure 57: Acylase activity on catheter.

The enzymatic activity of acylase when incorporated into the LbL film on catheters was determined at three different parts of the catheter. The ribbed part (the inflatable balloon) appears to be the most active one.

Figure 58 shows the activity of amylase on catheters. Again amylase showed more activity when incorporated in the LbL film together with acylase. When both enzymes were used for the LbL assembly, the smooth part of the catheter shows the highest activity. The ribbed part shows in both cases the lowest activity.

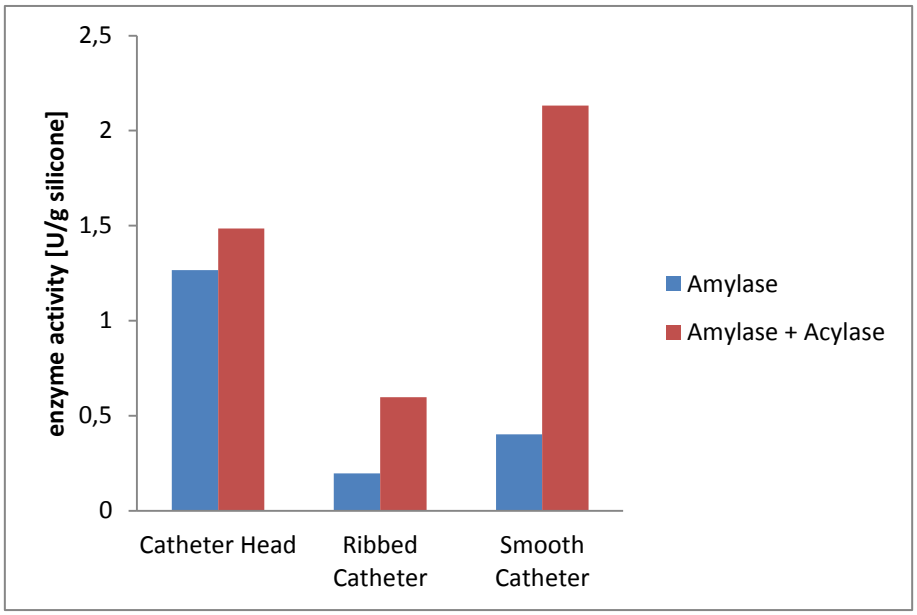

Figure 58: Amylase activity on catheter.

The enzymatic activity of amylase when incorporated into the LbL film on catheters alone and alternately with acylase was determined at three different parts of the catheter. Again amylase showed more activity when the LbL assembly was performed with both enzymes, then the smooth part appears to be the most active one.

So both enzymes could be successfully integrated in the LbL film on catheters and kept their activity.

For all activity assays on silicone or catheter supports it is important to notice, that the enzyme activities are given per g or mg of silicone substrate and not as specific enzymatic activity. An important next step will be to determine the amount of protein, that is bound on the silicone after a LbL assembly to determine the specific enzyme activity. Then it will be possible to compare the activity and the kinetics of the free and “bound” enzymes and calculate the percentage of activity loss. Then the whole LbL approach can be optimized to reach the highest specific enzyme activities.

5.2 Dynamic biofilm inhibition test

5.2.1 Bacterial adhesion test

There were no colonies visible on any of the cetrimide agar plates. Most probably the sonication step was too harsh and all adherent bacteria were killed in this step.

5.2.2 Microscopy

The following pictures are from the microscopy of the catheter cross-sections after the dynamic biofilm test. Always two cross-sections per sample were analysed and the pictures are divided into the outer part and the inner part of the cross-section ring. Figure 59 shows pictures from the catheter control. The whole sample showed bacterial growth as well as other contaminations.

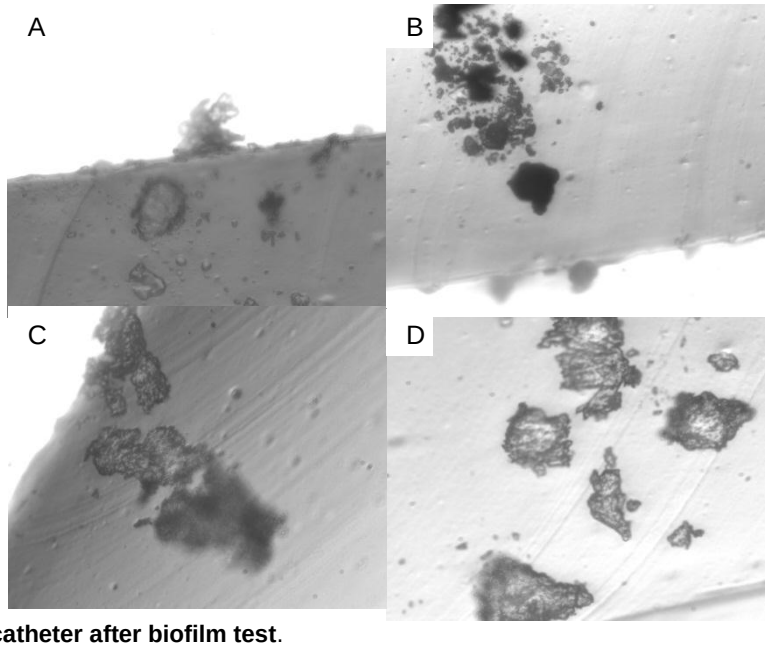

Figure 59: Blank catheter after biofilm test.

Microscopy picture of the cross-section of a blank catheter after a biofilm test with *P. aeruginosa*. The whole sample showed bacterial growth and other contaminations. A and B: outer part of ring; C and D: inner part of ring; Magnification: x 40; Exposure time: 1.6 ms

As seen in figure 60, figure 61 and figure 62 all the LbL coated samples gave the impression of having less bacteria and being cleaner compared to the catheter control.

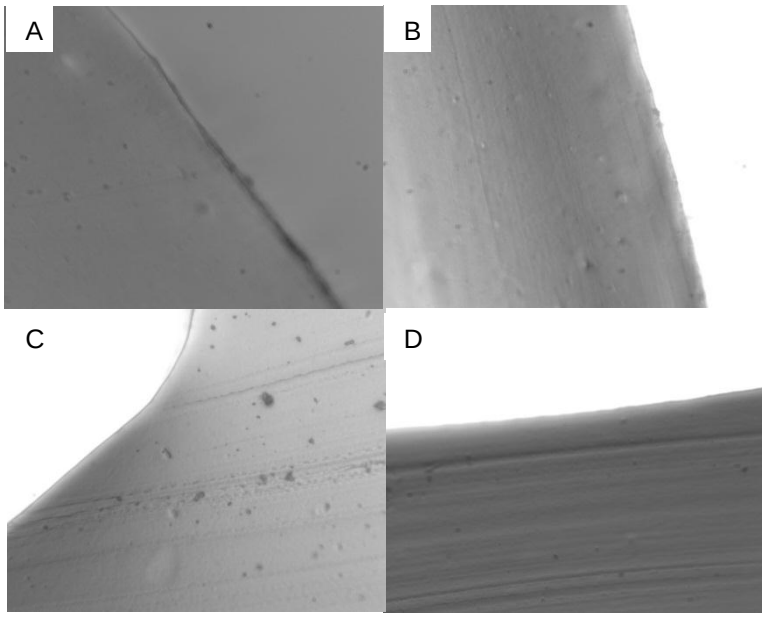

Figure 60: LbL acylase catheter after biofilm test.

Microscopy picture of the cross-section of a LbL acylase catheter after a biofilm test with *P. aeruginosa*. The whole sample appears clean and without bacterial growth. A and B: outer part of ring; C and D: inner part of ring Magnification: x 40; Exposure time: 1.6 ms

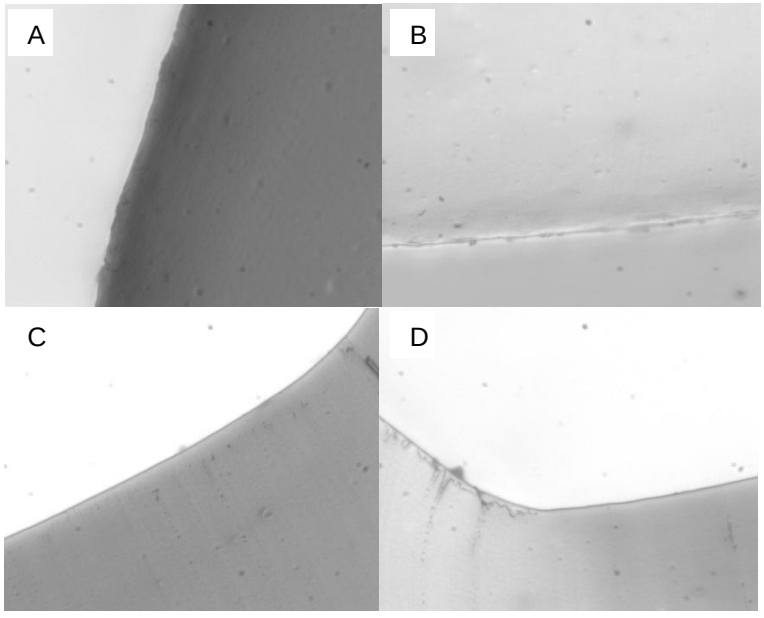

Figure 61: LbL amylase catheter after biofilm test.

Microscopy picture of the cross-section of a LbL amylase catheter after a biofilm test with *P. aeruginosa*. The whole sample appears clean and without bacterial growth. A and B: outer part of ring; C and D: inner part of ring Magnification: x 40; Exposure time: 1.6 ms

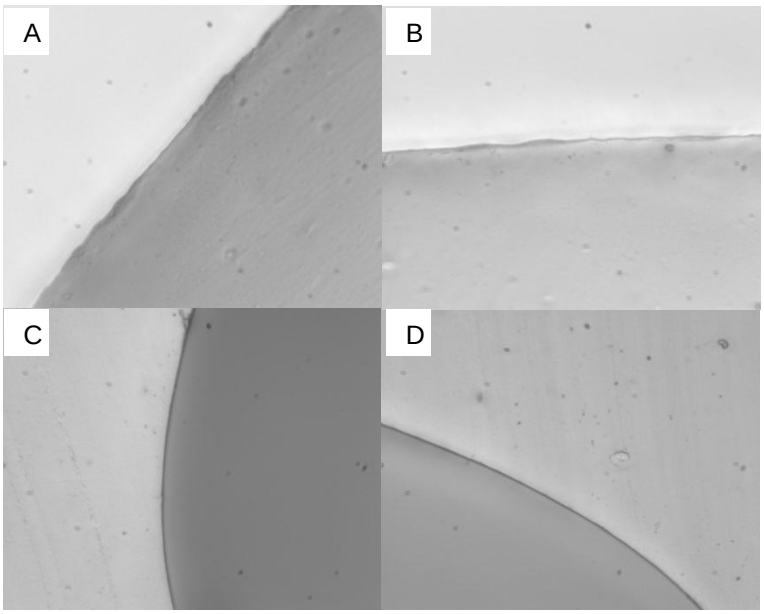

Figure 62: LbL acylase + amylase catheter after biofilm test.

Microscopy picture of the cross-section of a LbL acylase+ amylase catheter after a biofilm test with *P. aeruginosa*. The whole sample appears clean and without bacterial growth. A and B: outer part of ring; C and D: inner part of ring Magnification: x 40; Exposure time: 1.6 ms

As this dynamic biofilm test was only performed once, more experiments have to be done and they have to be analysed more specific to gain more concrete results. For example the bacterial adhesion test could be repeated with some modifications to enable the counting of the attached bacteria.

Anyhow, at the moment it seems that bioactive multilayer coatings with acylase and amylase can inhibit biofilm formation on catheters and investigations should be continued.

V. Conclusion and Outlook

In this study two enzymes, namely acylase and α-amylase, were attached onto silicone films to achieve a bioactive multilayer coating. Both free enzymes (acylase and α-amylase) were found to be able to inhibit the biofilm formation of *P. aeruginosa* and *E. coli*, as proven by a 96-well plate assay. The inhibition mechanism of acylase on *E. coli* biofilm formation is not yet clear and should be further investigated. Nevertheless, these enzymes were further attached to the silicone surface in a LbL-fashion. Untreated silicone as well as APTES functionalised silicone was used for the construction of these LbL films.

The successful build-up of these multilayer films on silicone and on APTES silicone was proven by different methods. Changes in water contact angle, appearing amide I bands and hydrogen bonding bands on FTIR spectra as well as fluorescence microscopy of FITC labelled enzymes suggest that the film assembly was successful.

The fluorescence microscopy pictures of the labelled enzymes showed, that the layers on APTES silicone are more tightly compared to the untreated silicone.

No major changes were observed on the FTIR spectra and water contact angle after a 24 hours washing step in DI H_2O at 37°C, which leads to the assumption that the film is stable and cannot be washed away easily.

The remaining activity of both enzymes in LbL films on silicone was proven by specific assays. Acylase also shows activity on LbL APTES silicone, but for amylase there was no activity detectable on LbL APTES silicone. This could be due to the fact, that the layers on APTES silicone are more tightly and therefore steric hindrance might be a problem. Activity assays of LbL samples after 24 h washing in DI H_2O at 37 °C and after storage for one week at room temperature were performed and suggest that the activity of the enzymes on silicone is maintained.

Summarising these results, the basic principle of enzyme based anti-biofilm silicone coatings was clearly proven.

So after performing the same LbL build-up on catheters a dynamic biofilm inhibition test was done. In this test all our LbL coated catheters gave the impression of being cleaner, and having less bacteria compared to the control catheter. Due to a lack of

time this dynamic biofilm test was only performed once, so more experiments have to be done.

But due to these promising results it seems that bioactive coatings with acylase and α-amylase could be a solution to avoid biofilm formation on medical indwelling devices and the investigations should be on-going.

Further investigations should include for example the determination of the amount of enzyme that is integrated in the LbL film to compare the specific enzyme activities of immobilised and free enzyme. Furthermore the LbL build-up can be optimised according towards highest specific enzyme activity. After optimising the LbL assembly the dynamic biofilm tests should be repeated and analysed in more detail.

To make sure that these materials can be used in the human body, toxicity tests with human cells should also be one of the future steps.

VI. List of figures, tables and equations

VII. Bibliography

[1]. **Rabih, O. and Darouiche, M.D.** Treatment of Infections Associated with Surgical Implants. *N. Engl. J. Med.* 2004, Vol. 350, 1422-1429.

[2]. **Davies, D.** Understanding biofilm resistance to antibacterial agents. *Nat. Rev. Drug. Discov.* 2003, Vol. 2, 114-122.

[3]. **Mah, T.-F.C. and O'Toole, G.A.** Mechanisms of biofilm resistance to antimicrobial agents. *TRENDS in Microbiology.* 2001, Vol. 9, 1.

[4]. **Ha, U-S. and Cho, Y.-H.** Catheter-associated urinary tract infections: new aspects of novel urinary catheters. *International Journal of Antimicrobial Agents .* 2006, Vol. 28, 485-490.

[5]. **Kowalczuk, D., Ginalska, G. and Golus, J.** Characterization of the developed antimicrobial urological catheters. *International Journal of Pharmaceutics.* 2010, Vol. 402, 175-183.

[6]. **Wright, Gerard D.** Q&A: Antibiotic resistance: where does it come from and what can we do about it? *BMC Biology.* 2010, Vol. 8, 123.

[7]. **Aehle, Wolfgang.** *Enzymes in Industry: Production and Application.* leiden : Wiley-VCH, 2007. 978-3-527-31689-2.

[8]. **O'Toole, G., Kaplan, H.B. and Kolter, R.** Biofilm formation as microbial development. *Annu Rev Micobiol.* 2000, Vol. 54, 49-79.

[9]. **Costerton, J. W., Stewart, Philip S. and Greenberg, E. P.** Bacterial Biofilms: A Common Cause of Persistent Infections. *Science.* 1318, 1999, Vol. 284.

[10]. **Costerton J.W. et al.** Microbial biofilms. *Annual Reviews in Microbiology.* 1995, Vol. 49.

[11]. **De Beer, D., Stoodley, P. and Lewandowski, Z.** Liquid Flow and Mass Transport in heterogeneous biofilms. *Biotech.Bioeng.* 1996, Vol. 30, 2761-2765.

[12]. **Davie, D.G., Chakrabarty, A.M. and Geesey, G. G.** Exopolysaccharide Production in Biofilms: Substratum Activation of Alginate Gene Expression by Pseudomonas aeruginosa. *Applied and environmetal microbiology.* 1993, Vol. 59, 4.

[13]. **Fux, C.A., et al.** Survival strategies of infectious biofilms. *Trends Microbiol.* 2005, Vol. 13, 34-40.

[14]. **Stamm, W. E.** Catheter-associated urinary tract infections: epidemiology, pathogenesis, and prevention. *Am. J. Med.* 1991, Vol. 91, 65-71.

[15]. **Morris, N.S., Stickler, D.J. and McLean, R.J.** The development of bacterial biofilms on indwelling urethral catheters. *World J. Urol.* 1999, Vol. 17, 345-350.

[16]. **Davenport, K. and Keeley, F.X.** Evidence for the use of silver-alloy-coated urethral catheters. *J. Hosp. Infect.* 2005, Vol. 60, 298-303.

[17]. **Stark, R.P. and Maki, D.G.** Bacteriuria in the catheterized patient. *N Engl J Med.* 1984, Vol. 311, 560-564.

[18]. **Cochrane, D. M. G. and al., et.** *J. Med. Microbiol.* 1988, Vol. 27, 255.

[19]. **Khoury, A. E., et al.** *Am.Soc. Artif. Intern. Organs J.* 1992, Vol. 38, 174.

[20]. **Jass, J., Surman, S. and Walker, J. T.** *Medical biofilms: detection, prevention, and control.* s.l. : John Wiley & Sons, Ltd. ISBN: 0-471-98867-7, 2003.

[21]. **O'Toole, G., Kaplan, H.B. and Kolter, R.** BIOFILM FORMATION AS MICROBIAL DEVELOPMENT. *Annu. Rev. Microbiol. .* 2000, Vol. 54, 49-79.

[22]. **Pamp, S.J., Gjermansen, M. and Tolker-Nielsen, T.** The Biofilm Matrix: A Sticky Framework. [book auth.] S. Kjelleberg and M. Givskov. *The biofilm mode of life Mechanisms and Adaptions.* s.l. : horizon bioscience, 2007.

[23]. **Zhang, Lian-Hui and Dong, Yi-Hu.** Quorum sensing and signal interference: diverse implications. *Molecular Microbiology.* 2004, Vol. 53(6), 1563-1571.

[24]. **Atkinson, Steve and Williams, Paul.** Quorum sensing and social networking in the microbial world. *Journal of the royal society.* 2009, Vol. 6, 959-578.

[25]. **Cámara, M., Williams, P. and Hardman, A.** Controlling infection by tuning in and turning down the volume of bacterial small-talk. *Lancet Infectious Diseases.* 2002, Vol. 2, 667-676.

[26]. **Williams, P.** Quorum sensing, communication and cross-kingdom signalling in the bacterial world. *Microbiology.* 2007, Vol. 153, 3923-3938.

[27]. **Nealson, K.H., Plarr, T. and Hastings, J.W.** Cellular control of the synthesis and activity of the bacterial luminescent system. *Journal of Bacteriology.* 1970, Vol. 104, 313-322.

[28]. **Eberhard, A., et al.** Strucutral identification of autoinducer of Photobacterium fischeri luciferase. *Biochemistry.* 1981, Vol. 20, 2444-2449.

[29]. **Whitehead, N.A., et al.** Quorum sensing in Gram-negative bacteria. *FEMS Microbiology Review.* 2001, Vol. 25, 365-404.

[30]. **Fuqua, C. and Greenberg, E.P.** Listening in on bacteria: acyl-homoserine lactone signalling. *Nature Review Molecular Cell Biology.* 2002, Vol. 3, 685-695.

[31]. **Engebrecht, J., Nealson, K.H. and Silverman, M.** Bacterial bioluminescence: isolation and genetic analysis of the functions from Vibrio fischeri. *Cell.* 1983, Vol. 32, 773-781.

[32]. **Kaplan, H.B. and Greenberg, E.P.** Diffusion of autoinducer is involved in regulation of the Vibrio fischeri luminescence system. *Journal of Bacteriology.* 1985, Vol. 163, 1210-1214.

[33]. **Devine, J.H., Shadel, G.S. and Baldwin, T.O.** Identification of the operator of the lux regulon from the Vibrio fischeri strain ATCC7744. *Proc. Natl. Acad. Sci. USA .* 1989, Vol. 86, 5688-5692.

[34]. **Egland, K.A. and Greenberg, E.P.** Quorum sensing in Vibrio fischeri: elements of the luxI promoter. *Molecular Microbiology.* 1999, Vol. 31(4), 1197–1204.

[35]. **Gambello, M.J. and Iglewski, B.H.** Cloning and characterization of the Pseudomonas aeruginosa lasR gene, a transcriptional activator of elastase expression. *Journal of Bacteriology.* 1991, Vol. 173, 3000-3009.

[36]. **Passador, L., et al.** Expression of Pseudomonas aeruginosa virulence genes requires cell-to-cell communication. *Science.* 1993, Vol. 260, 1127-1130.

[37]. **Toder, D.S., Gambello, M.J. and Iglewski, B.H.** Pseudomonas aeruginosa LasA: a second elastase under the transcriptional control of lasR. *Molecular microbiology.* 1991, Vol. 5, 2003-2010.

[38]. **Gambello, M.J., Kaye, S. and Iglewski, B.H.** LasR of Pseudomonas aeruginosa is a transcriptional activator of the alkaline protease gene (apr) and an

enhancer of exotoxin A expression. *Infection and Immunity.* 1993, Vol. 61, 1180-1184.

[39]. **Jones S, Yu B, Bainton NJ, Birdsall M, Bycroft BW, Chhabra SR, Cox AJ, Golby P, Reeves PJ, Stephens S, et al.** The lux autoinducer regulates the production of exoenzyme virulence determinants in Erwinia carotovora and Pseudomonas aeruginosa. *EMBO Journal.* 1993, Vol. 12, 2477-2482.

[40]. **Seed, P.C., Passador, L. and Iglewski, B.H.** Activation of the Pseudomonas aeruginosa lasI Gene byLasR and the Pseudomonas Autoinducer PAI: an Autoinduction Regulatory Hierarchy. *Journal of Bacteriology.* 1995, Vol. 177, 654-659.

[41]. **Pearson, J.P., et al.** A second N-acylhomoserine lactone signal produced by Pseudomonas aeruginosa. *Proc. Natl. Acad. Sci. USA.* 1995, Vol. 92, 1490-1494.

[42]. **Ochsner, U.A., et al.** Isolation and characerization of a regulatory gene afflecting rhamnolipid biosurfactan synthesis in Pseudomonas aeruginosa. *Journal of Bacteriology.* 1994, Vol. 176, 2044-2054.

[43]. **Köhler, T., et al.** Swarming of Pseudomonas aeruginosa is dependent on cell-to-cell signaling and requieres flagella and pili. *Jounral of Bacteriology.* 2000, Vol. 182, 59990-5996.

[44]. **Pesci, E.C., et al.** Regulation of las and rhl quorum sensing in Pseudomonas aeruginosa. *Journal of Bacteriology.* 1997, Vol. 179, 3127-3132.

[45]. **Van Houdt, R., et al.** N-acyl-L-homoserine lactone signal interception by Escherichia coli. *FEMS Microbiology Letters.* 2006, Vol. 256, 83-89.

[46]. **Ahmer, Brian M. M.** Cell-to-cell signalling in Escherichia coli and Salmonella enterica. *Molecular Microbiology .* 2004, Vol. 52, 933–945.

[47]. **Xavier, K. B. and Bassler, B.M.** LuxSquorum sensing: more than just a numbers game. *Current Opinion in Microbiology.* 2003, Vol. 6, 191-197.

[48]. **Stickler DJ, Morris NS, McLean RJ, Fuqua C.** Biofilms on indwelling urethral catheters produce quorum-sensing signal molecules in situ and in vitro. *Applied environmental Microbiology.* 1998, Vol. 64, 3486-3490.

[49]. **McClean, R.J.C., et al.** Evidence of autoinducer activity on naturally occurring biofilms. *FEMS Microbiology Letters.* 1997, Vol. 154, 259-263.

[50]. **Hentzer, M. and Giskov, M.** Pharmacological inhibition of quorum sensing for the treatment of chronic bacterial infections. *The Journal of Clinical Investigation.* 2003, Vol. 112, 1300-1307.

[51]. **Jones, S.M., Dang, T.T. and Martinuzzi, R.** Use of quorum sensing antagonists to deter the formation of crystalline Proteus mirabilis biofilms. *International Journal of Antimicrobial Agents.* 2009, Vol. 34, 360-364.

[52]. **McLean, R.J., Pierson, LS 3rd and Fuqua, C.** A simple screening protocol for the identification of quorum signal antagonists. *J Microbiol Methods.* 2004, Vol. 58 (3), 351-360.

[53]. **Hoang, T.T. and Schweizer, H.P.** Characerization of Pseudomonas aeruginosa enoyl-acyl carrier protein reductase (FabI): a target for the antimicrobial triclosan and its role in acylated homoserine lactone synthesis. *Journa of Bacteriology.* 1999, Vol. 181, 5489-5497.

[54]. **Löffler, G.** *Basiswissen Biochemie mit Pathobiochemie.* s.l. : Springer-Lehrbuch, 2001. 3-540-67389-X.

[55]. **Decher, G.** Fuzzy Nanoassemblies: Toward Layered Polymeric Multicomposites. *Science.* 1997, Vol. 227, 1232-1237.

[56]. **Tang, Z., et al.** Biomedical Applications of Layer-by-Layer Assembly: From Biomimetics to Tissue Engineering. *Advanced Materials.* 2006, Vol. 18, 3203-3224.

[57]. **Ariga, K., Hill, J.P. and Ji, Q.** Layer-by-layer assembly as a versatile bottom-up nanofabrication technique for exploratory research and realistic application. *Physical Chemistry Chemical Physics.* 2007, Vol. 9, 2319-2340.

[58]. **Schrier, Robert W.** *Diseases of the kidney and urinary tract.* Philadelphia : Lippincott Williams & Wilkins, 2007. 978-0-7817-9307-0.

[59]. **Jones , G.Ll., et al.** A Strategy for the Control of Catheter Blockage by Crystalline Proteus mirabilis Biofilm Using the Antibacterial Agent Triclosan. *European Urology.* 2005, Vol. 48, 838-845.

[60]. **Chothia, Cyrus.** Principles that determine the structure of proteins. *Ann. Rev. Biochem.* 1984, Vol. 53, 537-572.

[61]. **Gallagher, Warren.** *FTIR Analysis of Protein Structure.*

[62]. **Wong, S.Y., et al.** Drastically Lowered Protein Adsorption on Microbicidal Hydrophobic/Hydrophilic Polyelectrolyte Multilayers. *Biomacromolecules.* 2012, Vol. 13, 719-726.

[63]. **Monroe, D.** Looking for Chinks in the Armor of Bacterial Biofilms. *PLoS Biology.* 2007, Vol. 5, 11.

[64]. **Pearson, J.P., et al.** Structure of the autoinducer required for expression of Pseudomonas aeruginosa virulence genes. *Proc.Natl.Acad.Sci USA.* 1994, Vol. 91, 197-201.

[65]. **Alikhajeh, J., et al.** Structure of Bacillus amyloliquefaciens α-amylase at high resolution: implications for thermal stability. *Acta Crystallogr Sect F Struct Biol Cryst Commun.* 2010, Vol. 66, 121-129.